



Universiteit
Leiden
The Netherlands

Novel role of the AT-HOOK MOTIF NUCLEAR LOCALIZED 15 gene in Arabidopsis meristem activity and longevity

Rahimi, A.

Citation

Rahimi, A. (2020, September 1). *Novel role of the AT-HOOK MOTIF NUCLEAR LOCALIZED 15 gene in Arabidopsis meristem activity and longevity*. Retrieved from <https://hdl.handle.net/1887/136334>

Version: Publisher's Version

License: [Licence agreement concerning inclusion of doctoral thesis in the Institutional Repository of the University of Leiden](#)

Downloaded from: <https://hdl.handle.net/1887/136334>

Note: To cite this publication please use the final published version (if applicable).

Cover Page



Universiteit Leiden



The handle <http://hdl.handle.net/1887/136334> holds various files of this Leiden University dissertation.

Author: Rahimi, A.

Title: Novel role of the AT-HOOK MOTIF NUCLEAR LOCALIZED 15 gene in Arabidopsis meristem activity and longevity

Issue Date: 2020-09-01

Chapter 2

A suppressor of axillary meristem maturation promotes longevity in flowering plants

Omid Karami¹, Arezoo Rahimi¹, Majid Khan^{1,5}, Marian Bemer³, Rashmi R. Hazarika⁴, Patrick Mak^{1,6}, Monique Compier^{1,7} Vera van Noort^{2,4} and Remko Offringa^{1,*}

Nature Plants (2020)

¹ Plant Developmental Genetics and ² Bioinformatics and Genomics, Institute of Biology Leiden, Leiden University, Sylviusweg 72, 2333 BE Leiden, The Netherlands

³ Laboratory of Molecular Biology and B.U. Bioscience, Wageningen University & Research, Droevendaalsesteeg 1, 6708 PB Wageningen, The Netherlands

⁴ KU Leuven, Centre of Microbial and Plant Genetics, Kasteelpark Arenberg 20, B-3001 Leuven, Belgium.

⁵ Present address: Institute of Biotechnology and Genetic Engineering (IBGE), University of Agriculture Peshawar, Peshawar, Pakistan

⁶ Present address: Sanquin Plasma Products BV, Dept. Product Development, Plesmanlaan 125, 1066 CX Amsterdam, The Netherlands

⁷ Present address: Rijk Zwaan, Burgemeester Crezeelaan 40, 2678 KX De Lier, The Netherlands

* Email: r.offringa@biology.leidenuniv.nl

Abstract

Post embryonic development and longevity of flowering plants are for a large part determined by the activity and maturation state of stem cell niches formed in the axils of leaves, the so-called axillary meristems (AMs) (Grbić and Bleecker, 2000; Wang et al., 2018). The genes that are associated with AM maturation and underlie the differences between monocarpic (reproduce once and die) annual and the longer-lived polycarpic (reproduce more than once) perennial plants are still largely unknown. Here we identify a new role for the Arabidopsis *AT-HOOK MOTIF CONTAINING NUCLEAR LOCALIZED 15* (*AHL15*) gene as a suppressor of AM maturation. Loss of *AHL15* function accelerates AM maturation, whereas ectopic expression of *AHL15* suppresses AM maturation and promotes longevity in monocarpic Arabidopsis and tobacco. Accordingly, in Arabidopsis grown under longevity-promoting short day conditions, or in polycarpic *Arabidopsis lyrata*, expression of *AHL15* is upregulated in AMs. Together our results indicate that *AHL15* and other *AHL* clade-A genes play an important role, directly downstream of flowering genes (*SOC1*, *FUL*) and upstream of the flowering promoting hormone gibberellic acid, in suppressing AM maturation and extending the plant's lifespan.

Keywords: Axillary meristems (AMs), *AHL* genes, monocarpic, polycarpic, *Arabidopsis*, tobacco

Introduction

Plant architecture and -longevity are dependent on the activity of stem cell groups called meristems. The primary shoot and root apical meristem of a plant are established during early embryogenesis and give rise to respectively the shoot- and the root system during post-embryonic development. In flowering plants, post-embryonic shoot development starts with a vegetative phase, during which the primary shoot apical meristem (SAM) produces morphogenetic units called phytomers consisting of a stem (internode) subtending a node with a leaf and a secondary or axillary meristem (AM) located in the axil of the leaf (Grbić and Bleecker, 2000; Wang et al., 2018). Both the SAM and these AMs undergo a maturation process. Like the SAM, young immature AMs are vegetative and when activated they produce leaves, whereas in plant species such as *Arabidopsis* partially matured AMs produce a few cauline leaves before they fully mature into inflorescence meristems (IMs) and start developing phytomers comprising a stem subtending one or more flowers (Park et al., 2014; Wang et al., 2018).

The maintenance of vegetative development after flowering is an important determinant of plant longevity and -life history. Monocarpic plants, such as the annuals *Arabidopsis thaliana* (*Arabidopsis*) or *Nicotiana tabacum* (tobacco), complete their life cycle in a single growing season. The AMs that are established during the vegetative phase initially produce leaves. Upon floral transition, however, all AMs rapidly convert into IMs producing secondary and tertiary inflorescences with bracts and flowers, thus maximizing offspring production before the plant's life ends with senescence and death. The number of leaves and bracts produced by an AM is thus a measure for its maturation state upon activation. By contrast, many other flowering plant species are polycarpic perennials, such as the close *Arabidopsis* relative *Arabidopsis lyrata*. Under permissive growth conditions, they can live and flower for more than two growing seasons. As some AMs are maintained in the vegetative state, this allows polycarpic plants to produce new shoots after seed set and the subsequent activation of these AMs by the appropriate growth conditions before the start of the next growing season (Munné-Bosch, 2008; Amasino, 2009). Despite considerable interest in the molecular basis of plant life history, the proposed molecular mechanisms determining the difference in loss or maintenance of vegetative development after flowering between respectively monocarpic or polycarpic plants are still largely based on our extensive knowledge on the control of flowering in *Arabidopsis* and closely related species. From these studies, the MADS box proteins SUPPRESSOR OF OVEREXPRESSION OF CONSTANS 1 (SOC1) and FRUITFULL (FUL) have been identified as key promoters of flowering and monocarpic growth, and FLOWERING LOCUS C (FLC) as their upstream cold-sensitive inhibitor (Melzer et al., 2008; Amasino, 2009; Kiefer et al., 2017). However, the factors that maintain vegetative development after flowering, and thereby allow polycarpic growth, are still elusive.

Here we present evidence that the *Arabidopsis AT-HOOK MOTIF COINTAINING NUCLEAR LOCALIZED 15 (AHL15)* gene plays an important role in the control of AM maturation and extending the plant's lifespan.

Results and discussion

AHL15 forms a clade (clade-A) with 14 other *AHL* genes in Arabidopsis that encode nuclear proteins containing a single N-terminal DNA binding AT-hook motif and a C-terminal Plants and Prokaryotes Conserved (PPC) domain (Supplementary Fig. 1a and Fig. 1a). The PPC domain was previously shown to contribute to the physical interaction with other AHL or nuclear proteins (Zhao et al., 2013). *AHL15* homologs have been implicated in several aspects of plant growth and development in Arabidopsis, including hypocotyl growth and leaf senescence (Street et al., 2008; Xiao et al., 2009; Zhao et al., 2013), flower development (Ng et al., 2009), and flowering time (Xiao et al., 2009; Yun et al., 2012).

In contrast to other *ahl* mutants (Xiao et al., 2009), *ahl15* loss-of-function mutant plants (Supplementary Fig. 1b-e) flowered at the same time and developed the same number of rosette leaves before flowering as wild-type plants, both under short day (SD) and long day (LD) conditions (Fig. 1d,e). After bolting, however, the AMs located in the axils of rosette leaves (rosette AMs) of *ahl15* mutant plants produced less additional rosette leaves compared to those in wild-type plants (Fig. 2a,e and Fig. 3a-c). More detailed analysis showed that this reduction in additional rosette leaf production in *ahl15* plants was not caused by a delayed outgrowth of rosette AMs into axillary buds or to early floral transition, but rather to a reduction in the vegetative activity of these buds (Fig. 4a,b). Following the floral transition, the *ahl15* rosette AMs produced the same number of cauline leaves (Fig. 3d) and flowers (Supplementary Fig. 2a) as the wild type (Col-0). However, the cauline branches produced by the aerial AMs on *ahl15* inflorescences developed less cauline leaves (Fig. 3e) and flowers/fruits (Supplementary Fig. 2b) compared to those produced by wild-type inflorescences, resulting in a significant reduction of the total number of cauline leaves and flowers on *ahl15* inflorescences. Introduction of the *pAHL15:AHL15* genomic clone into the *ahl15* mutant background restored both the rosette and cauline leaf as well as the flower and fruit numbers to wild-type levels (Fig. 2e and Fig 3a-e, Supplementary Fig. 2b), confirming that the phenotypes were caused by *ahl15* loss-of-function. GUS staining of plants carrying a *pAHL15:GUS* promoter:reporter fusion showed that *AHL15* is expressed in AMs (Fig. 2b,c) and young axillary buds (Fig. 2d). Together these results suggested a novel role for *AHL15* in controlling AM maturation.

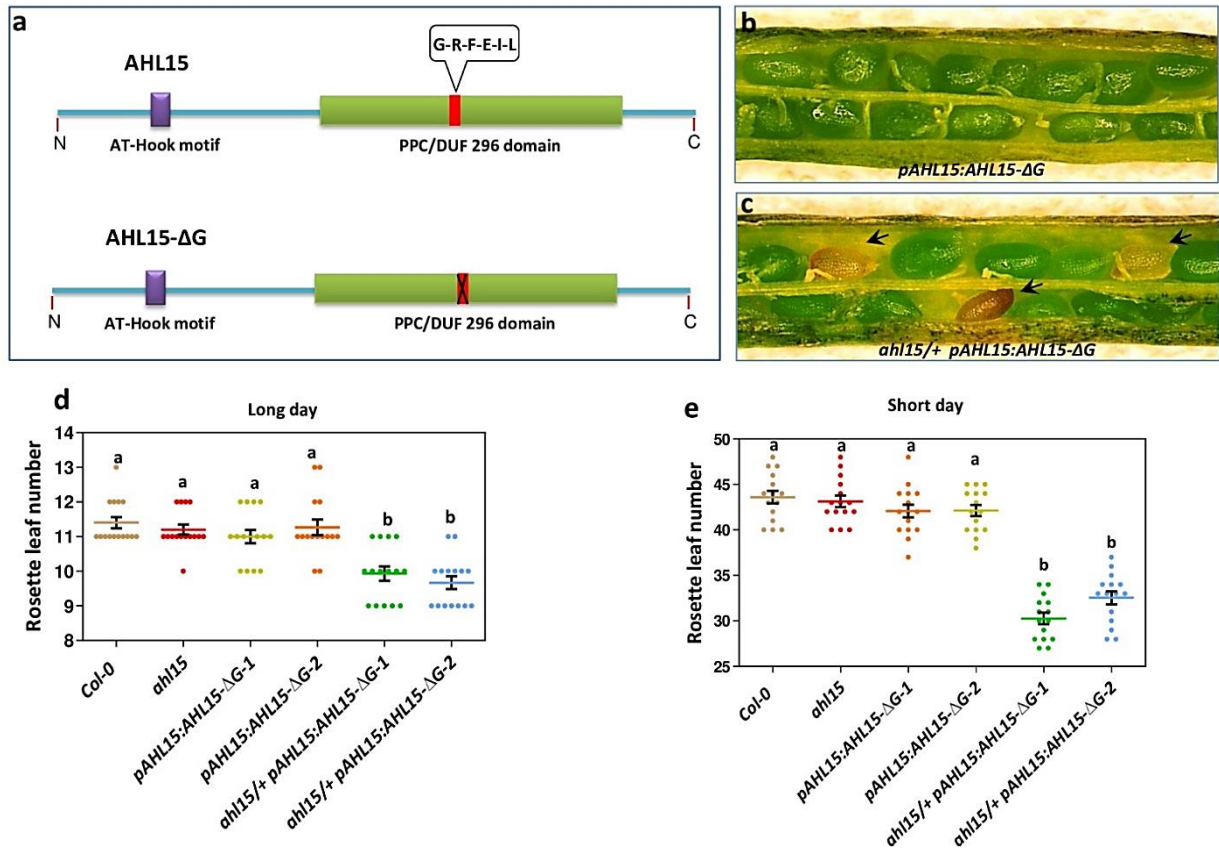


Fig. 1| Expression of a dominant negative AHL15-ΔG mutant protein. Expression of a dominant negative AHL15-ΔG mutant protein in the Arabidopsis *ahl15* mutant background causes early flowering and impairs seed development. **a**. The schematic domain structure of AHL15 and the dominant negative AHL15-ΔG version, in which six-conserved amino-acids (Gly-Arg-Phe-Glu-Ile-Leu, red box) are deleted from the C-terminal PPC domain. **b**. Wild-type seed development in *pAHL15:AHL15-ΔG* siliques. **c**. Aberrant seed development (arrowheads) in *ahl15/+ pAHL15:AHL15-ΔG* siliques (observed in 3 independent *pAHL15:AHL15-ΔG* lines crossed with the *ahl15* mutant). Similar results were obtained in three independent experiments. **d**, **e**. The number of rosette leaves produced by the SAM in wild-type, *ahl15*, *pAHL15:AHL15-ΔG* and *ahl15/+ pAHL15:AHL15-ΔG* plants grown in long day (LD, **d**) or short day (SD, **e**) conditions. Two independent transgenic lines (1 and 2) were used in each experiment. Dots in **d** and **e** indicate the rosette leaf number per plant (n=15 biologically independent plants), horizontal lines the mean and error bars the s.e.m. Letters (a, b, c) indicate statistically significant differences ($P < 0.01$), as determined by a one-way ANOVA with a Tukey's HSD post hoc test.

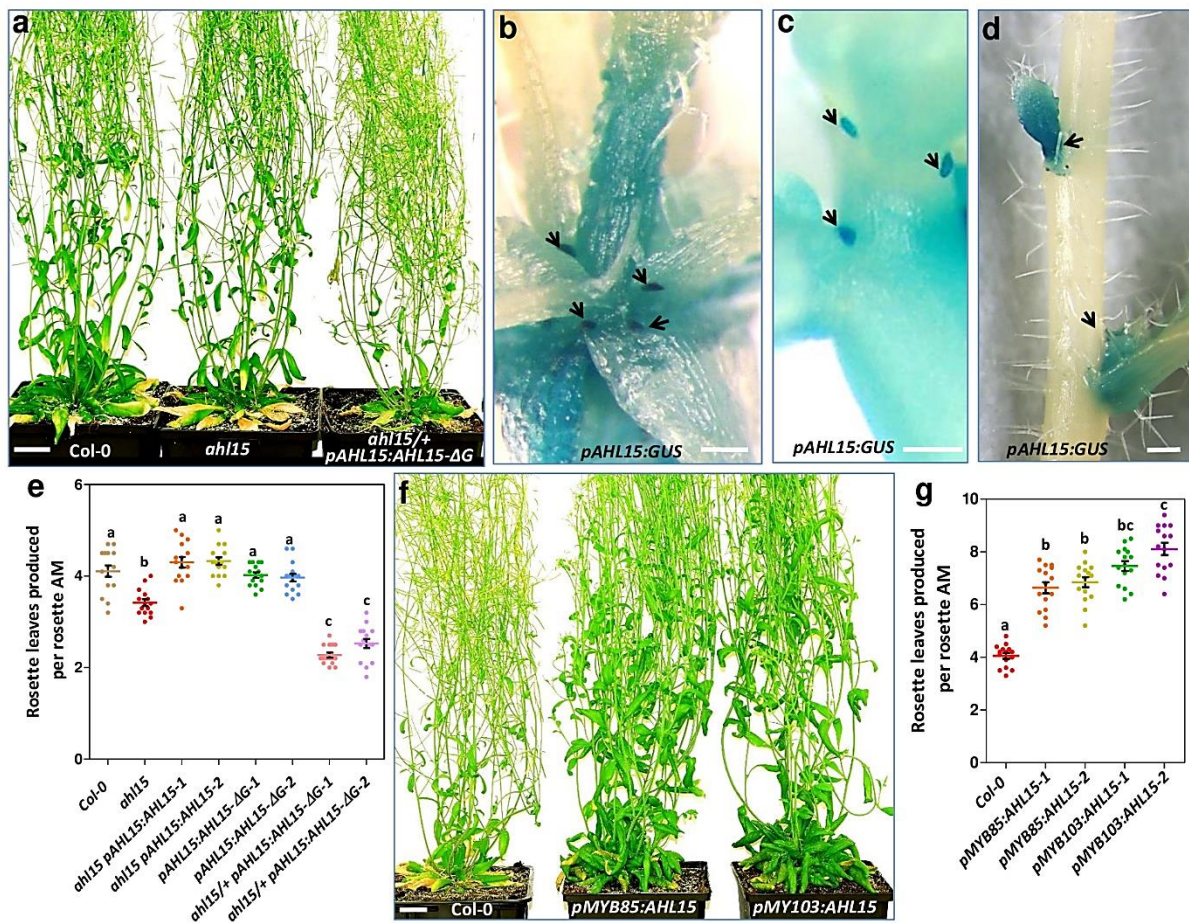


Fig. 2 | *AHL15* represses AM maturation in Arabidopsis. (a) Shoot phenotypes of fifty-day-old flowering wild-type (left), *ah15* (middle) and *ah15/+ pAHL15:AHL15-ΔG* mutant (right) plants. (b-d) *pAHL15:GUS* expression in rosette AMs (arrow heads in b), aerial AMs located on a young inflorescence stem (arrow heads in c) and in activated axillary buds on an inflorescence stem (arrow heads in d) of a flowering plant. (e) The rosette leaves produced per rosette AM in fifty-day-old wild-type, *ah15*, *ah15 pAHL15:AHL15*, *pAHL15:AHL15-ΔG* and *ah15/+ pAHL15:AHL15-ΔG* plants. (f) Shoot phenotype of a sixty-day-old flowering wild-type (left), *pMYB85:AHL15* (middle) or *pMYB103:AHL15* (right) plant. (g) The rosette leaves produced per rosette AM in sixty-day-old wild-type, *pMYB85:AHL15* or *pMYB103:AHL15* plants. Dots in e and g indicate the number of rosette leaves per plant (n=15 biologically independent plants) per line, horizontal lines indicate the mean, and error bars the SEM. Letters (a, b, c) indicate statistically significant differences ($p < 0.01$), as determined by a one-way ANOVA with a Tukey's HSD post hoc test. The P values are provided in Supplementary Tables 3 and 4. Plants were grown under long day conditions (LD). Size bars indicate 2 cm in a, f and 1 mm in b-c. The leaf production per rosette AM in e and g was determined for two independent transgenic lines (1 and 2).

A suppressor of axillary meristem maturation promotes longevity in flowering..

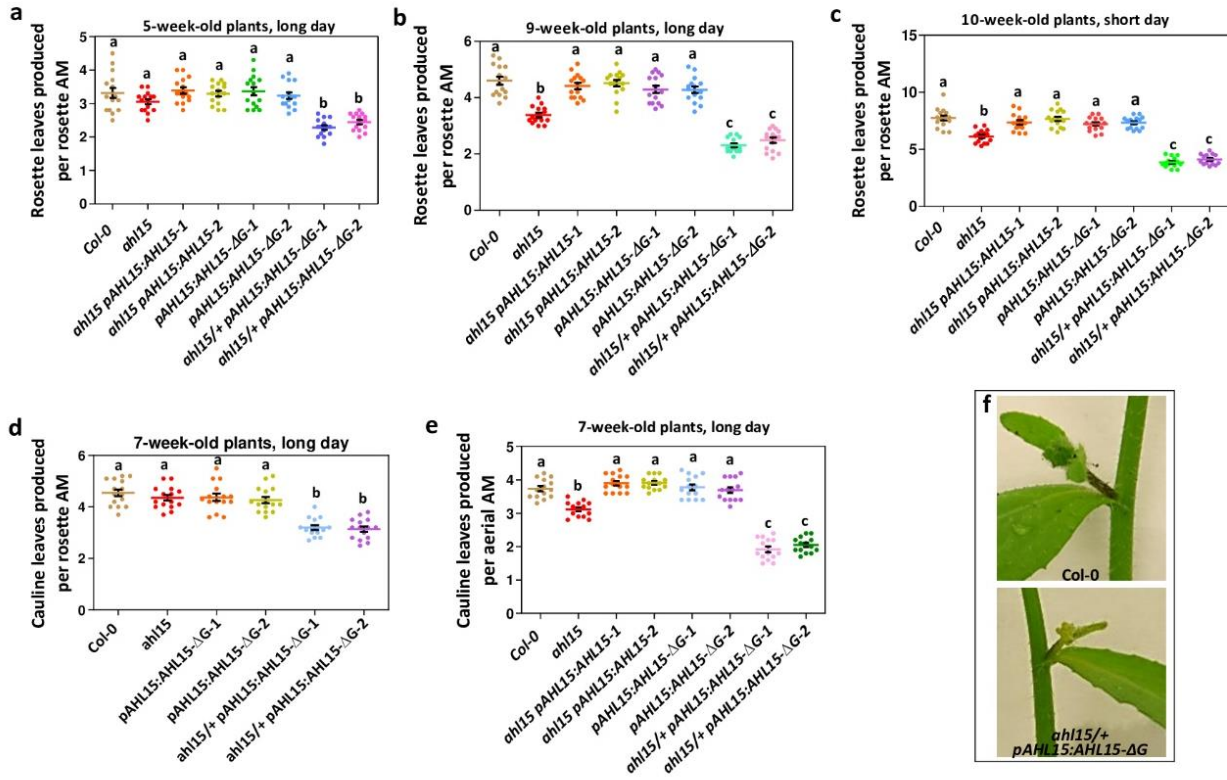


Fig. 3 | *AHL15* and other clade A *AHL* genes represses AM maturation in Arabidopsis. a, b. The number of rosette leaves produced per rosette AM of wild-type, *ahl15*, *ahl15 pAHL15:AHL15*, *pAHL15:AHL15-ΔG* and *ahl15/+ pAHL15:AHL15-ΔG* plants 5 (a), 9 (b), or 10 weeks (c) after germination in long day (LD, a,b) or short day (SD, c) conditions. **d, e.** The number of cauline leaves produced by rosette AMs (d) or by aerial AMs (e) of 7-week-old wild-type, *ahl15*, *ahl15 pAHL15:AHL15*, *pAHL15:AHL15-ΔG* and *ahl15/+ pAHL15:AHL15-ΔG* plants. Dots in a-e indicate rosette or cauline leaf number per AM per plant (n=15 biologically independent plants), horizontal lines the mean, and error bars the s.e.m. Letters (a, b, c) indicate statistically significant differences ($P < 0.01$), as determined by a one-way ANOVA with a Tukey's HSD post hoc test. The P values are provided in Supplementary Tables 8–12. **f.** A lateral inflorescence with cauline leaves formed on the first inflorescence node of a wild-type (top) or *ahl15/+ pAHL15:AHL15-ΔG* plant (bottom).

AHL proteins interact with each other through their PPC domain and with other non-AHL proteins through a conserved six-amino-acid (GRFEIL) region in the PPC domain. Expression of an AHL protein without the GRFEIL region leads to a dominant negative effect, as it generates a non-functional complex that is unable to modulate transcription (Zhao et al., 2013). Expression of a deletion version of AHL15 lacking the GRFEIL region under control of the *AHL15* promoter (*pAHL15:AHL15-ΔG*) in the wild-type background (n=20) resulted in fertile plants (Fig. 1a,b) that showed normal AM maturation (Fig. 2e and Fig. 3). In the heterozygous *ahl15* loss-of-function background, however, *pAHL15:AHL15-ΔG* expression induced early flowering (Fig. 1d,e, Fig. 4b), resulting in a strong reduction of rosette and cauline leaf production by AMs (Fig. 2a,e, Fig. 3a-f, Fig. 4a). Homozygous *ahl15 pAHL15:AHL15-ΔG* progeny were never obtained, and defective seeds present in siliques of *ahl15/+ pAHL15:AHL15-ΔG* plants suggest that this genetic combination is embryo lethal (Fig. 1b,c). The significantly stronger phenotypes observed for *ahl15/+ pAHL15:AHL15-ΔG* plants are in line with the dominant negative effect of AHL15-ΔG expression overcoming the functional redundancy among Arabidopsis clade A AHL family members (Street et al., 2008; Xiao et al., 2009; Zhao et al., 2013)

Based on the observation that the flowering time and the number of rosette leaves before bolting was the same for wild-type and *ahl15* loss-of-function plants, but not for *ahl15/+ pAHL15:AHL15-ΔG* plants, we speculated that other AHL clade A family members are more active in the SAM, whereas AHL15 more strongly acts on AM maturation. To test this, we overexpressed a fusion protein between AHL15 and the rat glucocorticoid receptor under control of the constitutive Cauliflower Mosaic Virus 35S promoter (*p35S:AHL15-GR*). This rendered the nuclear import and thereby the activity of the ectopically expressed AHL15-GR fusion inducible by dexamethasone (DEX). Untreated *p35S:AHL15-GR* plants showed a wild-type phenotype (Fig. 5b,c), but after spraying flowering *p35S:AHL15-GR* plants with DEX, rosette AMs produced significantly more rosette and cauline leaves (Fig. 5a-c). Interestingly, spraying *p35S:AHL15-GR* plants before flowering also significantly delayed their floral transition (Fig. 5d), indicating that ectopically expressed AHL15 can also suppress maturation of the SAM. In turn, overexpression of the Arabidopsis AHL family members AHL19, AHL20, AHL27 and AHL29, as well as the putative AHL15 orthologs from *Brassica oleracea* and *Medicago truncatula* in Arabidopsis resulted in similar morphological changes as observed for *p35S:AHL15-GR* plants after DEX treatment. The overexpression plants produced more rosette and cauline leaves during flowering (Fig. 6a,b), supporting the idea that there is functional redundancy among AHL clade A family members and that the ability to control either SAM or AM maturation depends on the spatio-temporal expression of the corresponding genes.

In contrast to the observed growth arrest and death of two-month-old Arabidopsis plants grown under long day (LD) conditions (Fig. 7d), four-month-old short day (SD) grown Arabidopsis plants continued to grow after the first cycle of flowering, as aerial AMs on the last-formed lateral branches produced new rosette leaves (Fig. 7a and Fig. 8). However, SD grown *ahl15* mutant plants did not show this renewed vegetative growth and died, whereas *ahl15 pAHL15:AHL15* plants grew like wild type under these conditions (Fig. 7a and Fig. 8). GUS staining of *pAHL15:GUS* plants revealed that AHL15 expression was strongly enhanced in young lateral inflorescences, axils of cauline leaves and rosette branches in SD conditions

compared to LD conditions (Fig. 7b,c and Fig. 9), indicating that *AHL15* expression is day-length sensitive, and confirming the important role of this gene in extending the lifespan of *Arabidopsis* under SD conditions.

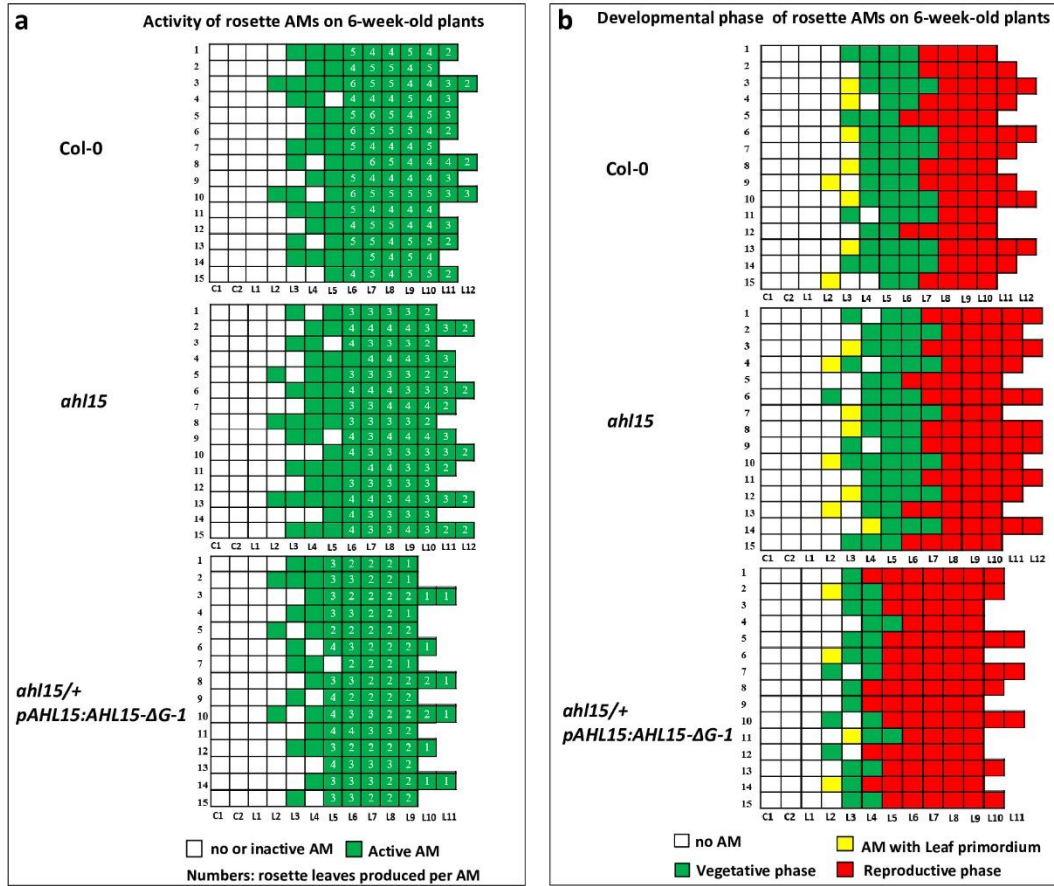


Fig. 4 | *Arabidopsis* *AHL* genes enhance the vegetative activity and suppress the floral transition of rosette AMs. **a.** Schematic representation of the vegetative activity of rosette AMs of six-week-old wild-type, *ah15* and *ah15/+ pAHL15:AHL15-ΔG-1* plants. Each row represents a single plant, and each square represents an individual AM in a cotyledon axil (C1 and C2) or in a rosette leaf axils (L1 to L12). The numbers within a square represent the number of rosette leaves produced by a rosette AM. A green square indicates a leaf axil with an active AM, as indicated by bud outgrowth or leaf development, and a white square indicates a leaf axil without an (active) AM. **b.** Developmental phase of the rosette AMs of six-week-old wild-type, *ah15* and *ah15/+ pAHL15:AHL15-ΔG-1* plants. White, yellow, green or red squares indicate axils without (active) AM, or rosette AMs with at least one visible leaf primordium, producing rosette leaves (vegetative) or producing cauline leaves or flowers (reproductive), respectively. Plants in **a** and **b** were grown in LD conditions.

Growing *Arabidopsis* plants under SD conditions significantly delays flowering (Andrés and Coupland, 2012), and this might thus indirectly enhance the repressing effect of *AHL15* on AM maturation and extending the lifespan. In order to assess *AHL15* function independently of day length and flowering time, we expressed *AHL15* under control of the *MYB85* or *MYB103* promoters, which are highly active in *Arabidopsis* rosette nodes and aerial axillary buds (Fig. 10a) (Ko et al., 2004). In LD conditions, *pMYB85:AHL15* and *pMYB103:AHL15* plants flowered at the same time as wild-type plants, but their AMs produced significantly more rosette and cauline leaves compared to those in wild-type plants (Fig. 2f,g and Fig. 10b,c). Moreover, after flowering and seed set, when wild-type plants senesced and died, *pMYB85:AHL15* and *pMYB103:AHL15* rosette and aerial AMs produced new rosette leaves, which allowed these plants to continue to grow and generate new flowers and seeds (Fig.

7d,e). Also senesced *p35S:AHLL15-GR* plants carrying fully ripened siliques started new aerial vegetative development on lateral secondary inflorescences after DEX treatment, and ultimately produced new inflorescences from the resulting rosettes (Fig. 11a). Interestingly, the development of vegetative shoots from AMs formed on rosette and aerial nodes after reproduction also contributes to the polycarpic growth habit of *Arabis alpina* or *Cardamine flexuosa* plants^{15,16}. Our results indicate that increased expression of *AHLL15* in late stages of development promotes longevity by inducing a polycarpic-like growth habit in Arabidopsis, with an important difference that AMs that remain vegetative do not show dormancy.

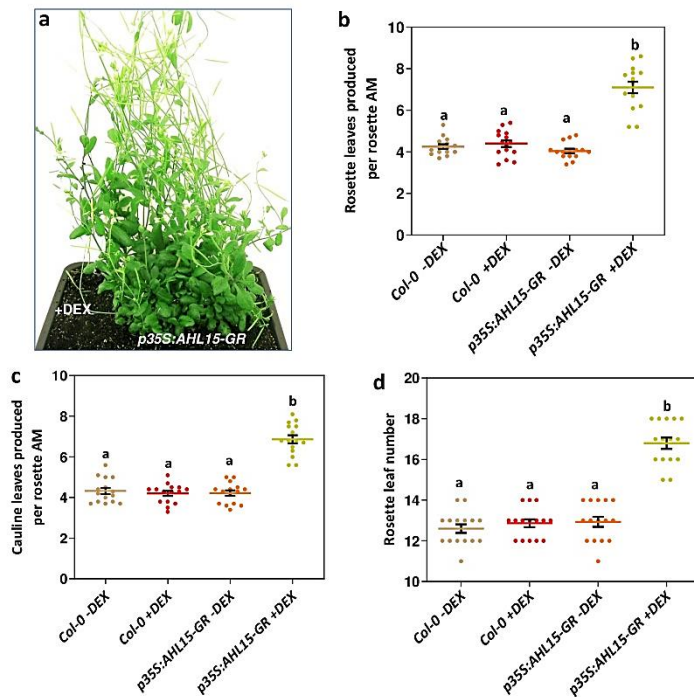


Fig. 5 | *AHLL15* overexpression delays floral transition of the SAM and represses AM maturation. **a.** Shoot phenotype of a flowering 7-week-old *35S:AHLL15-GR* plant that was DEX-treated upon bolting (5 weeks old). **b.** **c.** Number of rosette leaves (**b**) or cauline leaves (**c**) produced by rosette AMs of 7-week-old mock-treated wild-type, DEX-treated wild-type, mock-treated *35S:AHLL15-GR* and DEX-treated *35S:AHLL15-GR* plants. Plants were DEX-treated upon bolting (5 weeks old) and scored 2 weeks later. **d.** The number of rosette leaves produced by the SAM in mock-treated wild-type, DEX-treated wild-type, mock-treated *35S:AHLL15-GR* and DEX-treated *35S:AHLL15-GR* plants. Non-flowering (3-week-old) plants were treated and the SAM-produced rosette leaves were counted after bolting. Dots in **b-d** indicate number of leaves (per AM or SAM) per plant

($n=15$ biologically independent plants), horizontal lines the mean, and error bars the s.e.m. Letters (a, b, c) indicate statistically significant differences ($P < 0.01$), as determined by a one-way ANOVA with a Tukey's HSD post hoc test. Plants were grown in LD conditions.

To determine whether heterologous *AHLL15* expression could induce similar developmental changes in a monocarpic plant species from a different family, we introduced the *35S:AHLL15-GR* construct into tobacco. Wild-type and *p35S:AHLL15-GR* tobacco plants were allowed to grow and set seeds without DEX treatment. After seed harvesting, all leaves and side branches were removed, and the bare lower parts of the primary stems were either mock- or DEX treated. Whereas stems of wild-type and mock-treated *p35S:AHLL15-GR* plants did not show any growth, the AMs on DEX-treated *p35S:AHLL15-GR* tobacco stems resumed vegetative growth, eventually leading to a second cycle of flowering and seed set (Fig. 7f). Continued DEX treatment after each subsequent cycle of seed harvesting efficiently induced vegetative growth and subsequent flowering and seed set, allowing the *p35S:AHLL15-GR* tobacco plants to survive for more than 3 years (Fig. 11b). This result confirmed the conclusion from previous overexpression experiments (Fig. 7d,e, Fig. 5 and Fig. 11a) that enhanced *AHLL15* expression facilitates polycarpic-like growth by keeping some AMs in the vegetative state after flowering.

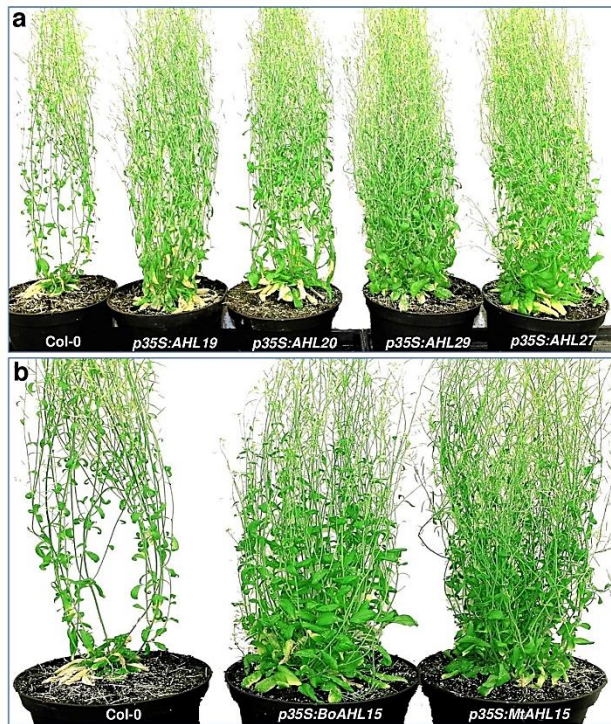


Fig. 6 | Overexpression of *Arabidopsis* AHL15 paralogs or putative orthologs represses AM maturation in *Arabidopsis*. Overexpression of *Arabidopsis* AHL15 paralogs or putative orthologs represses AM maturation in *Arabidopsis*. (a and b) Wild-type (Col-0) or transgenic 7-week-old *Arabidopsis* plants overexpressing *Arabidopsis* AHL19, AHL20, AHL27 and AHL29 (a), or the putative AHL15 orthologs from *Brassica oleracea* (BoAHL15) or *Medicago trunculata* (MAHL15) (b). For a and b similar results were obtained in two independent experiments. Plants were grown in LD conditions. For presentation purposes, the original background of the images was replaced by a homogeneous white background

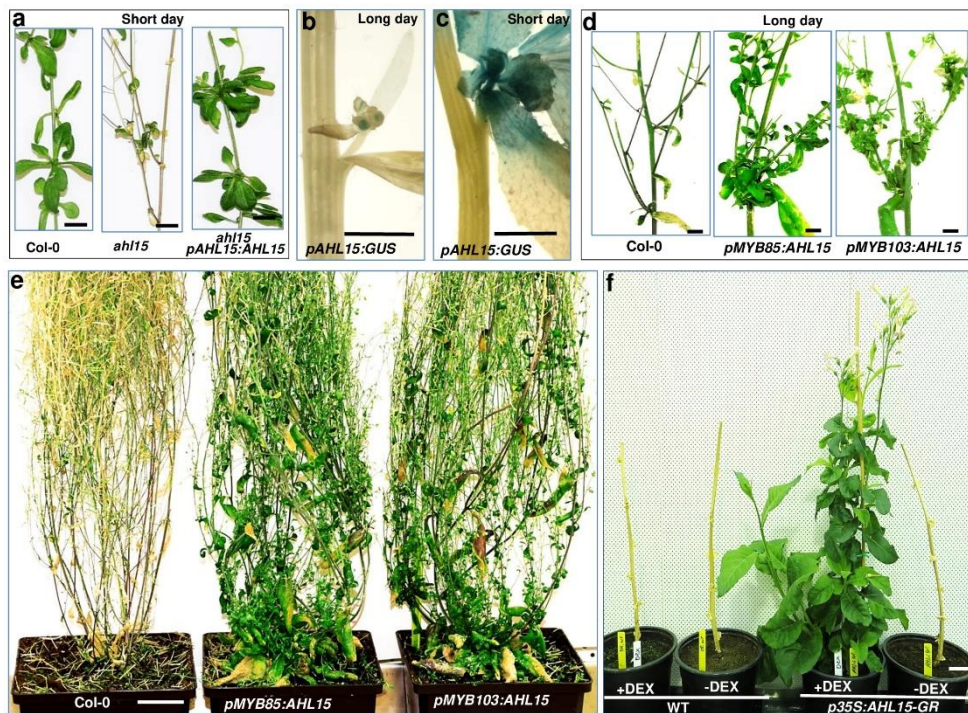


Fig. 7 | AHL15 promotes longevity in *Arabidopsis* and tobacco. a, Rosette leaves produced by aerial AMs in 4-month-old wild-type (left) and *ah15 pAHL15:AHL15* (right) plants, but not in *ah15* mutant plants (middle), grown under SD conditions. **b,c**, *pAHL15:GUS* expression in a lateral inflorescence of a 9-week-old plant grown under LD conditions (**b**) and a 4-month-old plant grown under SD conditions (**c**). **d**, Lateral aerial nodes without and with rosette leaves in 4-month-old wild-type (left), *pMYB85:AHL15* (middle) and *pMYB103:AHL15* (right) plants grown under LD conditions. **e**, Phenotype of 4-month-old wild-type (Col-0, left), *pMYB85:AHL15* (middle) and *pMYB103:AHL15* (right) plants grown under LD conditions. **f**, Growth response following DEX treatment in bare stems of 5-month-old wild-type (WT, left) and *35S:AHL15-GR* (right) tobacco plants grown under LD conditions. Scale bars, 1 cm in **a–d**, 2 cm in **b** and 5 cm in **e**.



Fig. 8 | *AHL15* enhances the longevity of short day-grown *Arabidopsis* plants. Phenotype of 5-month-old wild-type (Col-0, left), *ahl15* (middle) and *ahl15 pAHL15:AHL15* (right) plants. The plants were grown in SD conditions.

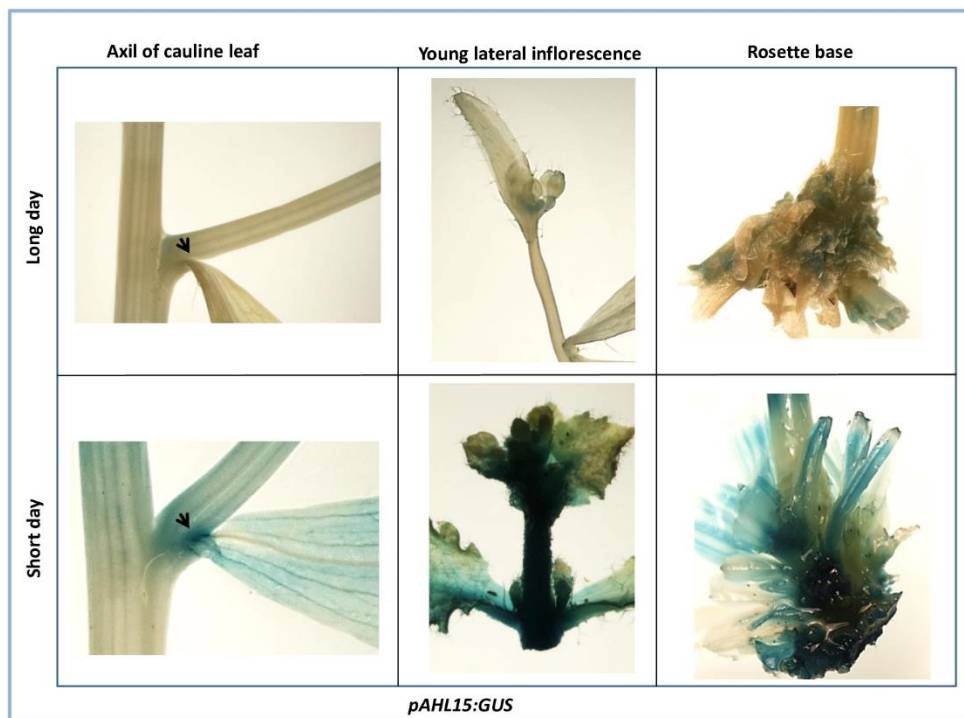


Fig. 9 | *AHL15* expression is day length sensitive. Expression of the *pAHL15:GUS* reporter in the axil of a cauline leaf (left, arrowheads), Young lateral inflorescence (middle) and rosette base (right) of a 9-week-old plant grown in LD conditions (top) or a 4-month-old plant grown under SD conditions (bottom). Similar results were obtained in two independent experiments.

A suppressor of axillary meristem maturation promotes longevity in flowering..

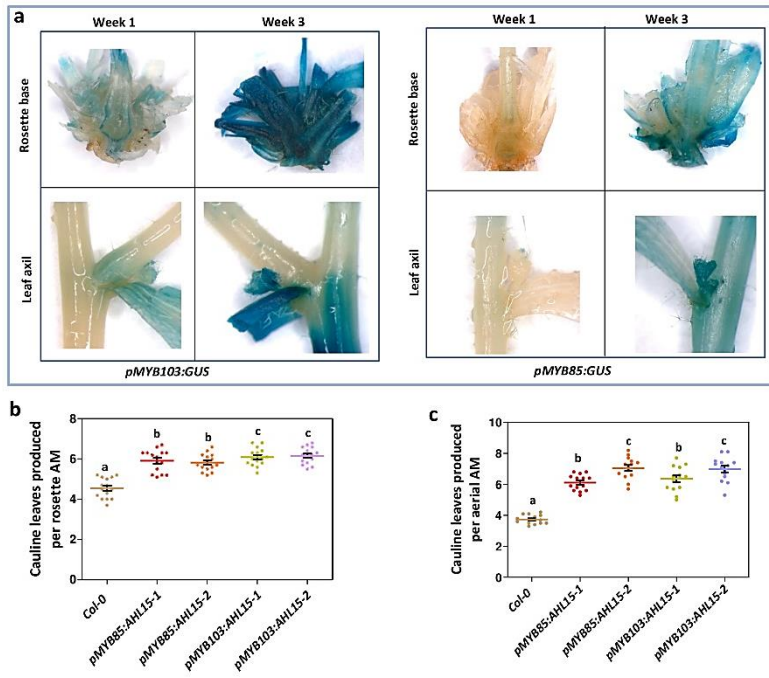


Fig. 10 | *AHL15* overexpression in the rosette base and leaf axils delays AM maturation in *Arabidopsis*. **a.** Expression of *pMYB58:GUS* and *pMYB103:GUS* reporters in the rosette base (top) or leaf axils (bottom) of *Arabidopsis* plants respectively one or three weeks after flowering, as monitored by histochemical GUS staining. **b, c.** The number of cauline leaves produced by rosette AMs (**b**) or aerial AMs (**c**) of 6-week-old (**b**) or 7-week-old (**c**) wild-type, *pMYB85:AHL15* or *pMYB103:AHL15* plants grown in LD conditions. Dots in **b** and **c** indicate number of cauline leaves produced per AM per plant (n=15 biologically independent plants), horizontal lines indicate the mean, and error bars the s.e.m. Letters (a, b, c) indicate statistically significant differences

($P < 0.01$), as determined by a one-way ANOVA with a Tukey's HSD post hoc test.

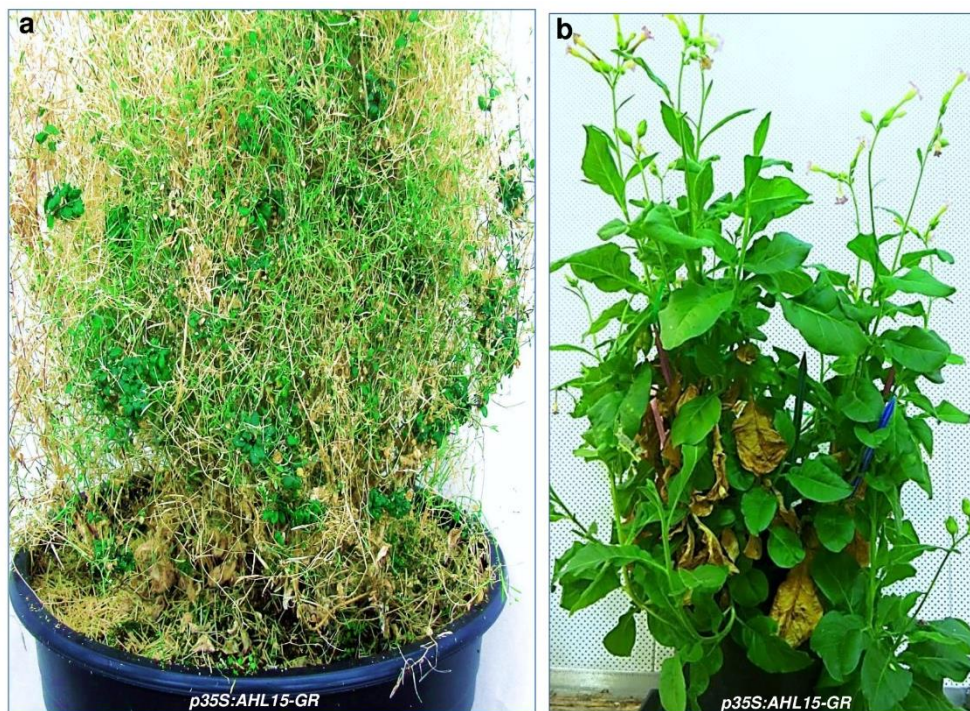


Fig. 11 | *AHL15* overexpression promotes longevity in *Arabidopsis* and tobacco. **a.** Renewed vegetative growth on aerial branches of a 5-month-old *Arabidopsis* 35S:AHL15-GR plant, 4 weeks after spraying with 20 μ M DEX. Similar results were obtained in three independent experiments. **b.** Efficient production of leaves and inflorescences in a 3-year-old 35S:AHL15-GR tobacco plant, 3 weeks after treatment with 30 μ M DEX, following 6 previous cycles of DEX-induced seed production. Plants in **a** and **b** were grown in LD condition.

Previously, loss-of-function of both *SOC1* and *FUL* in Arabidopsis was reported to suppress AM maturation, resulting in polycarpic-like growth (Melzer et al., 2008). We found that the aerial rosette formation that is normally observed in the *soc1 ful* double mutant was significantly reduced in *soc1 ful ahl15* triple mutant plants (Fig. 12a, b). Moreover, the polycarpic features of the *soc1 ful* double mutant were lost in the *ahl15* mutant background, as *soc1 ful ahl15* plants senesced and died following seed set, just like wild-type Arabidopsis. Expression analysis by qRT-PCR (Fig. 12c) or by using the *pAHL15:GUS* reporter (Fig. 12d,e) showed that *AHL15* was indeed strongly upregulated in *soc1 ful* inflorescence nodes and lateral inflorescences. Previous studies have revealed that the expression of *SOC1* is positively regulated by LD conditions. Moreover, *SOC1* was shown to bind to the *AHL15* upstream and downstream regions (Chr3, 20603158-20604316 and 20610947-20612012), which both contain a canonical CArG box (CC[A/T]6GG) (Fig. 12f) (Lee and Lee, 2010; Immink et al., 2012; Tao et al., 2012). This together with our own data suggested that *AHL15* expression is repressed by *SOC1* in LD conditions (Fig. 7b), and that unrepressed *AHL15* activity in the *soc1 ful* background explains the aerial rosette formation and the polycarpic-like growth of mutant plants. To check whether the CArG-box containing regions could also be bound by *FUL*, we used stem fragments containing axillary nodes of *pFUL:FUL-GFP ful* plants to perform ChIP. Subsequent qPCR revealed significant enrichment for the upstream and downstream regions (Fig. 12g), indicating that *FUL* can repress *AHL15* expression by directly binding to these regions. To further confirm that *FUL* and *SOC1* can bind the CArG-boxes in the *AHL15* up- and downstream regions, we performed Electrophoretic Mobility Shift Assay (EMSA) experiments. Probe fragments containing the corresponding regulatory regions (frag 1 and frag 3), or these regions with a mutated CArG-box (frags 1m and 3m), were tested with *SOC1* and *FUL* homo- and heterodimers. The *SOC1/FUL* heterodimer could bind to both regulatory fragments, but this binding was reduced when the CArG-box was mutated in frag 1m and even completely abolished in frag 3m (Fig. 12h), providing additional evidence for the importance of the CArG-boxes for the binding of *SOC1* and *FUL*. The *SOC1* homodimer showed the same results, while the *FUL* homodimer did not show binding (Supplementary Fig. 3).

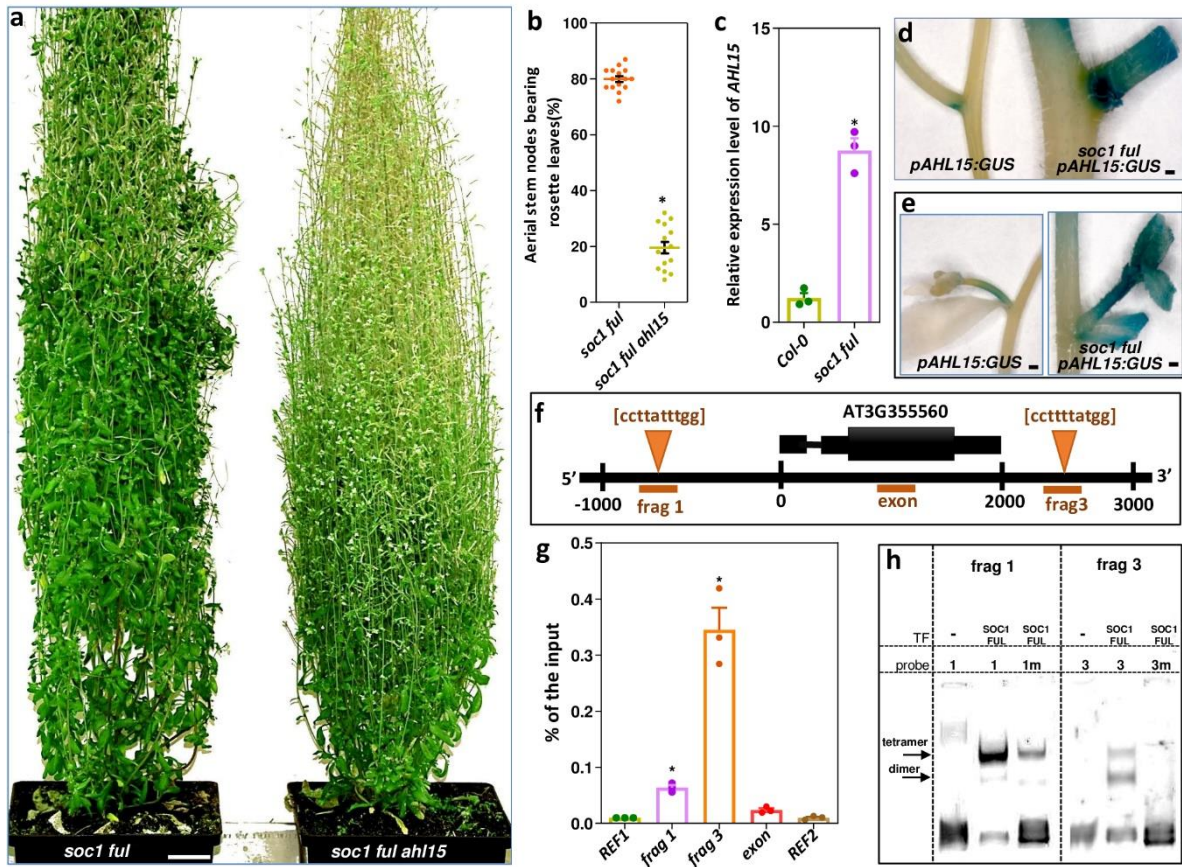


Fig. 12 | AHL15 is essential for suppression of AM maturation in the *Arabidopsis soc1 ful* mutant. **a**, A 3-month-old *soc1 ful* double-mutant plant with numerous aerial rosettes (left) and a *soc1 ful ahl15* triple-mutant plant with a limited number of aerial rosettes (right), both grown under LD conditions. **b**, Percentage of aerial stem nodes bearing rosette leaves in 3-month-old *soc1 ful* and *soc1 ful ahl15* plants. Dots indicate the percentage per plant ($n = 10$ biologically independent plants), horizontal lines the mean and error bars indicate s.e.m. The asterisk indicates a significant difference ($P < 0.001$) as determined by two-sided Student's t -test. **c**, qPCR analysis of *AHL15* expression in secondary inflorescence nodes of wild-type (Col-0) and *soc1 ful* plants 2 weeks after flowering. Dots indicate the values of three biological replicates per plant line, bars indicate the mean and error bars indicate s.e.m. The asterisk indicates a significant difference ($P < 0.001$) as determined by two-sided Student's t -test. **d,e**, *pAHL15:GUS* expression in an inflorescence node (**d**) and a secondary inflorescence (**e**) in wild-type (left) or a *soc1 ful* mutant (right) background. **f**, *AHL15* gene model with canonical CARG-boxes located in the upstream (frag 1) and downstream (frag 3) regions, but not in the exon fragment that was used as control (exon). The *AHL15* coding region is indicated by a thick black bar, exons by intermediate black bars and the position of the intron by a black line. **g**, Graph showing ChIP-qPCR results from *FUL-GFP ap1 cal* secondary inflorescence nodes using an anti-green fluorescent protein antibody. Enrichment of fragments was calculated as a percentage of the input sample. ref1 and ref2 are reference fragments (see Methods), while other fragments are also indicated in the gene model. Dots indicate the values of three biological replicates, bars the means and error bars indicate s.e.m. Asterisks indicate significant differences with ref1 and ref2 ($P < 0.001$) as determined by two-sided Student's t -test. Exact P values are provided in Supplementary Table 5. **h**, Binding of the transcription factors (TFs) SOC1 and FUL to regulatory regions near *AHL15*. Left: EMSA of promoter frag 1 with a wild-type (1) or mutated (m1) CARG-box. Right: EMSA of downstream frag 3 with a wild-type (3) or mutated (3 m) CARG-box. Shifting of the probe, indicating binding, occurred through either a tetramer (top band) or dimer (bottom band). Scale bars, 2 cm in **a** and 1 mm in **d,e**.

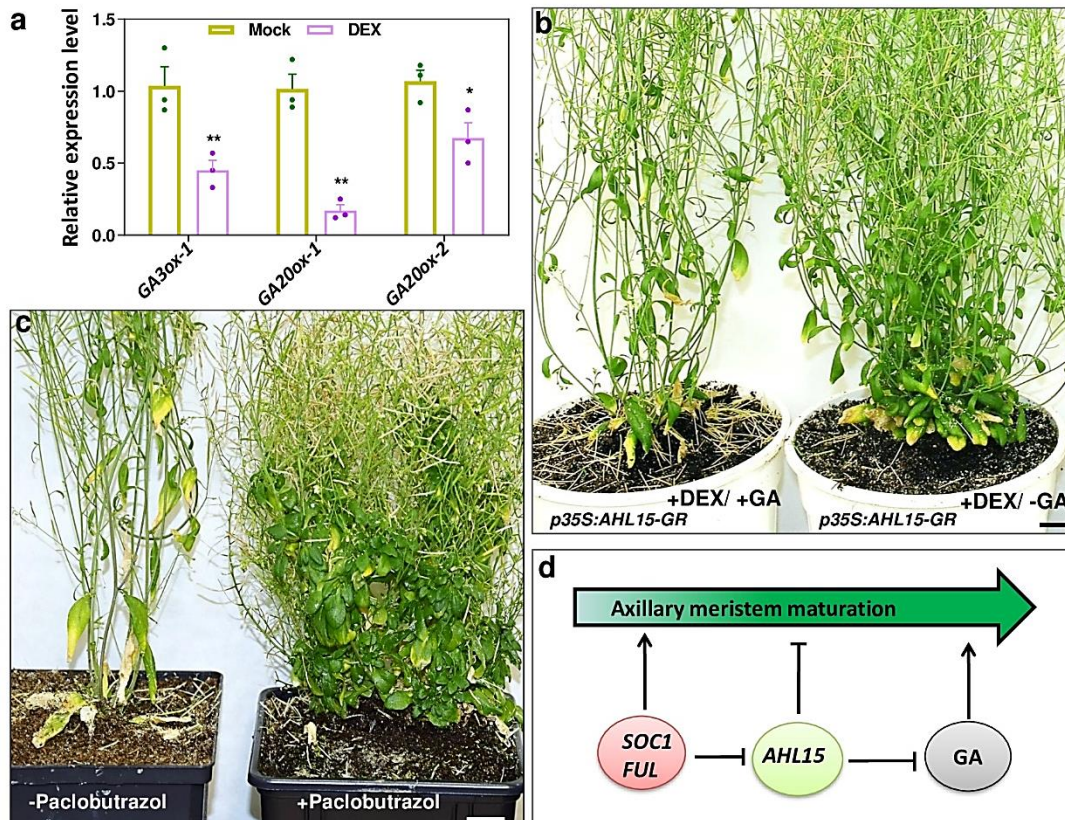


Fig. 13 | AHL15 delays AM maturation in part by suppression of GA biosynthesis. **a**, Relative expression level of GA biosynthesis genes *GA3OX1*, *GA20OX1* and *GA20OX2* by qPCR analysis in the basal regions of 1-week-old *35S:AHL15-GR* inflorescences 1 day after spraying with either water (mock) or 20 μ M DEX. Dots indicate the values of three biological replicates per plant line, bars indicate the mean and error bars indicate s.e.m. Asterisks indicate significant differences from mock-treated plants (* $P < 0.05$, ** $P < 0.01$), as determined by two-sided Student's *t*-test. **b**, Shoot phenotype of 3-month-old *p35S:AHL15-GR* plants that were DEX sprayed at 5 weeks of age and subsequently sprayed 1 week later with either 10 μ M GA4 (+GA) or water (-GA). **c**, Shoot phenotype of 3-month-old wild-type *Arabidopsis* plants that were sprayed 6 weeks earlier with either water (-Paclobutrazol) or 3 μ M paclobutrazol (+Paclobutrazol). Plants in **b,c** were grown under LD conditions; scale bars, 2 cm. **d**, Proposed model for the key role of *AHL15* (and other *AHL* clade-A genes) in controlling AM maturation downstream of flowering genes *SOC1* and *FUL* and upstream of GA biosynthesis. Blunt-ending lines indicate repression, arrows indicate promotion.

SOC1 and *FUL* are known as central floral integrators, as they integrate the different environmental and endogenous signaling pathways that influence flowering (Ko et al., 2004; Lee and Lee, 2010; Matsoukas et al., 2012). They promote flowering through activation of the floral meristem genes *APETALA1* (*API*) and *LEAFY* (*LFY*) (Turnbull, 2011; Song et al., 2013), and of genes involved in the biosynthesis of the plant hormone gibberellic acid (GA) (Andrés et al., 2014). GA plays an important role in the promotion of flowering through activation of *SOC1* and the *SQUAMOSA PROMOTER BINDING PROTEIN-LIKE* (*SPL*) genes (Yu et al., 2012; Wang, 2014). Interestingly, *AHL15* and *AHL25* also control GA biosynthesis by direct binding to the promoter of *GA3-oxidase1* (*GA3OX1*), which encodes an enzyme required for GA biosynthesis (Matsushita et al., 2007). We therefore investigated the relationship between GA biosynthesis and *AHL15* in the control of AM maturation. qPCR analysis showed that the expression of *GA3OX1*, *GA20OX1* and *GA20OX2*, genes, encoding rate limiting enzymes in the last steps of the GA biosynthetic pathway (Huang et

al., 1998; Rieu et al., 2008; Andrés et al., 2014), was down-regulated in DEX-treated *35S:AHL15-GR* inflorescence nodes (Fig. 13a). In line with the down-regulation of GA biosynthesis, GA application to DEX-treated flowering *p35S:AHL15-GR* plants resulted in a remarkable repression of vegetative AM activity (Fig. 13b). In turn, treatment of flowering wild-type *Arabidopsis* plants by paclobutrazol, a potent inhibitor of GA biosynthesis, prevented AM maturation, resulting in the aerial rosette leaf formation and enhanced longevity (Fig. 13c). Based on our findings, we postulate that *AHL15* acts downstream of *SOC1* and *FUL* as central repressor of AM maturation, and that *AHL15* prevents AM maturation in part by suppressing GA biosynthesis (Fig. 13d). Interestingly, the polycarpic behavior of *Arabis alpina* was shown to be based on age-dependent suppression of *AaSOC1* expression¹⁵ and GA levels (Tilmes et al., 2019) and, like in our model (Fig. 13d), *AHL* genes might also link these two regulatory pathways facilitating polycarpic growth in *Arabis alpina*.

The existence of both mono- and polycarpic species within many plant genera indicates that life history traits have changed frequently during evolution (Amasino, 2009). *AHL* clade-A gene families can be found in both monocarpic and polycarpic plant species (Supplementary Fig. 4a) (Zhao et al., 2014), and expression of the *AHL* clade-A gene family could therefore provide a mechanism by which a plant species attains a polycarpic growth habit. A comparison of the gene family size in representative species of 3 plant families did however not show significant gene deletion or duplication events linked to respectively the monocarpic or polycarpic growth habit (Supplementary Fig. 4b). This suggests that a switch from monocarpic to polycarpic habit or vice versa could possibly be mediated by a change in gene regulation.

To find support for this, we compared the *AHL* gene family of *Arabidopsis* with that of its close polycarpic relative *Arabidopsis lyrata* (Remington et al., 2015). The *A. thaliana* and *A. lyrata* genomes both encode 15 *AHL* clade-A proteins, among which the orthologous pairs can clearly be identified based on amino acid sequence identity (Supplementary Fig. 5). We hypothesized that the polycarpic habit of *A. lyrata* might be associated with enhanced *AHL* clade-A gene expression leading to the maintenance of basal AMs in the vegetative state during flowering (Fig. 14a). Expression analysis of individual *AHL* clade-A genes in *Arabidopsis* showed that the expression of the majority of these genes, including *AHL15*, *AHL19*, and *AHL20*, was decreased in rosette nodes of *A. thaliana* flowering plants compared to 2-week-old seedlings (Fig. 14b). In contrast, the expression of 5 members of the *AHL* gene family (*AHL15*, *AHL17*, *AHL19*, *AHL20* and *AHL27*) was significantly higher in rosette nodes of flowering *A. lyrata* plants compared to seedlings (Fig. 14c). These data are in line with our hypothesis and suggest that the different life-history strategies in *A. thaliana* and *A. lyrata* might be associated with the differential regulation of *AHL* genes in AMs.

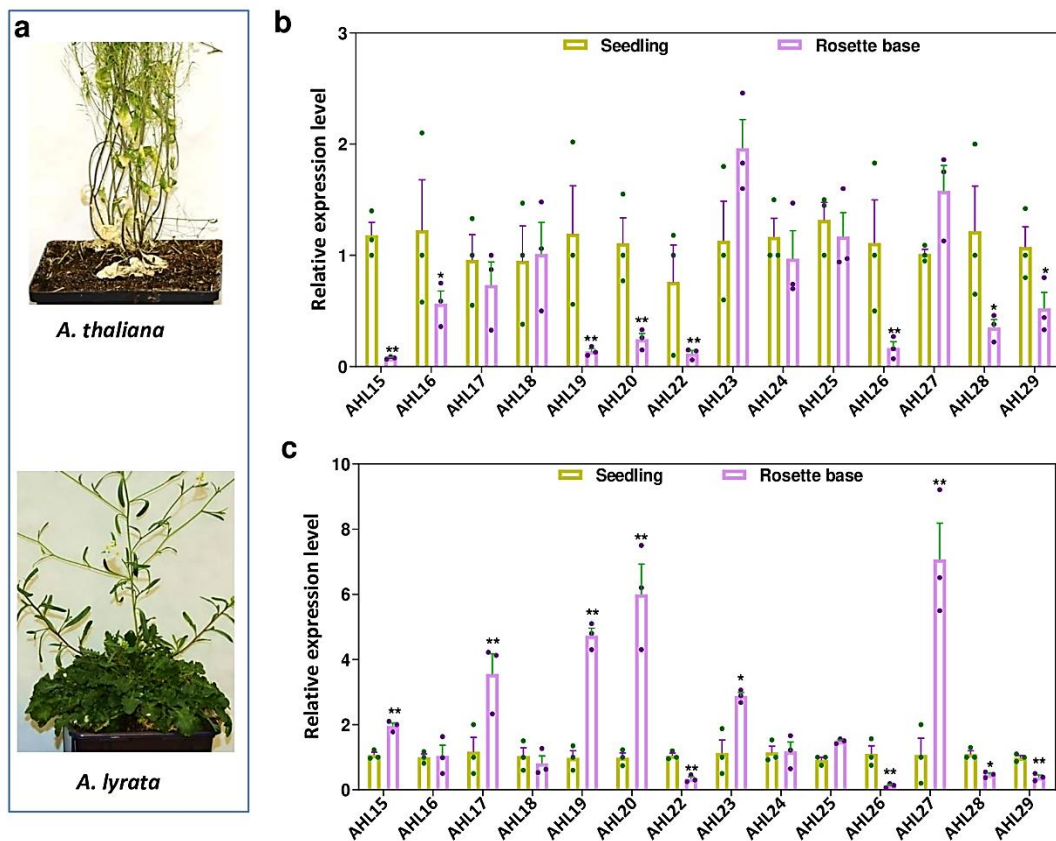


Fig. 14 | Expression of clade-A *AHL* genes in seedlings or in the rosette base of flowering *Arabidopsis* or *A. lyrata* plants. a. Shoot phenotype of a 3-month-old *Arabidopsis* (upper panel) or a 4-month-old *A. lyrata* (lower panel) plant grown in LD conditions. **b, c.** qPCR analysis of the expression of clade-A *AHL* genes in 2-week-old seedlings or in the rosette base of 2-month-old flowering plants of *A. thaliana* (**b**) or *A. lyrata* (**c**). Dots in **b** and **c** indicate relative expression levels per experiment ($n=3$ biologically independent replicates), bars indicate the mean, and error bars indicate the s.e.m. Asterisks indicate significant differences from mock-treated plants (* $p<0.05$, ** $p<0.01$, *** $p<0.001$), as determined by a two-sided Student's *t*-test.

Conclusion

In conclusion, our data provide evidence for a novel role for *AHL15* and other *AHL* clade-A genes in suppressing AM maturation and enhancing plant longevity. *Arabidopsis* plants with enhanced *AHL15* expression show polycarpic-like growth, but their vegetative AMs lack the dormancy that is characteristic for the reproductive cycles in perennial plants (e.g. *A. lyrata* and *A. alpina*). The importance of the SOC1/FUL-AHL-GA pathway in perennial life history therefore requires further confirmation. Although the exact mode of action of AHL proteins is largely unknown, they are characterized as DNA-binding proteins, and like AT-hook proteins in animals they seem to act through chromatin remodeling (Lim et al., 2007; Ng et al., 2009). It has been shown that *AHL22* represses *FLOWERING LOCUS T (FT)* expression by binding to the *FT* promoter where it possibly modulates the epigenetic signature around its binding region (Yun et al., 2012). Detailed studies on the chromatin configuration by approaches such as chromosome conformation capture technologies (Dekker et al., 2013)

should provide more insight into the mode of action of these plant-specific AT-Hook motif proteins. One of the objectives of our future research will be to unravel the molecular mechanisms by which these proteins influence plant development.

Methods

Plant material, growth conditions and phenotyping

All *Arabidopsis* mutant- and transgenic lines used in this study are in Columbia (Col-0) background. The *ahl15* (SALK_040729) T-DNA insertion mutant and the previously described *soc1-6 ful-7* double mutant (Wang et al., 2009) were obtained from the Nottingham *Arabidopsis* Stock Centre (NASC). Seeds were planted directly into soil in pots and germinated at 21°C, 65% relative humidity and a 16 hours (long day: LD) or 8 hours (short day: SD) photoperiod. When seedlings were 10 days old, they were thinned to one seedling per pot by cutting the hypocotyls. To score for phenotypes such as longevity, Col-0 wild-type, mutant or transgenic plants were transferred to larger pots about 3 weeks after flowering. *Nicotiana tabacum* cv SR1 Petit Havana (tobacco) plants were grown in medium-sized pots at 25°C, 70% relative humidity and a 16 hours photoperiod. For dexamethasone (DEX, Sigma-Aldrich) treatment, *Arabidopsis* and tobacco plants were sprayed with 20 and 30 µM DEX, respectively. To test the effect of GA on AHL15-GR activation by DEX treatment, 35-day-old flowering *p35S:AHL15-GR* plants were first sprayed with 20 µM DEX, followed 1 week later by spraying with 10 µM GA4 (Sigma-Aldrich). The production of rosette leaves, cauline leaves, flowers or fruits per rosette or aerial AM of 5-, 7-, 9- or 10-week-old plants was determined by dividing the total number of leaves or fruits produced by the number of active rosette or aerial AMs per plant. For the flowering time the number of rosette leaves produced by the SAM were counted upon bolting.

Plasmid construction and transgenic *Arabidopsis* lines

To generate the different *promoter:AHL15* gene fusions, the complete *AHL15* (AT3G55560) genomic fragment from ATG to stop codon was amplified from genomic DNA of *Arabidopsis* ecotype Columbia (Col-0) using PCR primers Gateway-AHL15-F and -R (Supplementary Table 1). The resulting fragment was inserted into pDONR207 via a BP reaction. LR reactions were carried out to fuse the *AHL15* coding region downstream of the 35S promoter in destination vector pMDC32 (Karimi et al., 2007). Subsequently, the 35S promoter was excised with *KpnI* and *SphI* and replaced by the Gateway cassette (*ccdB* flanked by *attP* sequences) amplified from pMDC164 (Karimi et al., 2007) by the *KpnI* and *SphI* flanked primers (Supplementary Table 1), resulting in plasmid pGW-AHL15. To generate the constructs *pFD:AHL15*, *pMYB85:AHL15*, *pMYB103:AHL15* and *pAHL15:AHL15*, 3 kb regions upstream of the ATG start codon of the genes *FD* (AT4G35900), *MYB85* (AT4G22680), *MYB103* (AT1G63910) and *AHL15* were amplified from ecotype Columbia (Col-0) genomic DNA using the forward (F) and reverse (R) PCR primers indicated in Supplementary Table 1. The resulting fragments were first inserted into pDONR207 by BP reaction, and subsequently cloned upstream of the *AHL15* genomic

fragment in destination vector pGW-AHL15 by LR reaction. To generate the *pAHL15:GUS*, *pMYB85:GUS* and *pMYB103:GUS* reporter constructs, the corresponding promoter fragments were cloned upstream of the *GUS* gene in destination vector pMDC164 by LR reaction. To generate the *pAHL15:AHL15-ΔG* construct, a synthetic *KpnI-SpeI* fragment containing the *AHL15* coding region lacking the sequence encoding the Gly-Arg-Phe-Glu-Ile-Leu amino acids in the C-terminal region (BaseClear, Leiden, NL) was used to replace the corresponding coding region in the *pAHL15:AHL15* construct. To construct *35S::AHL15-GR*, a synthetic *PstI-XhoI* fragment containing the *AHL15-GR* fusion (Shine Gene Molecular Biotech, see Supplementary File. 1) was used to replace the *BBM-GR* fragment in binary vector pSRS031 (Passarinho et al., 2008). To generate the other overexpression constructs, the full-length cDNA clones of *AHL19* (AT3G04570), *AHL20* (AT4G14465), *AHL27* (AT1G20900) and *AHL29* (AT1G76500) from *Arabidopsis* Col-0, *AC129090* from *Medicago trunculata* cv Jemalong (*MtAHL15*), and *Bo-Hook1* (AM057906) from *Brassica oleracea* var *alboglabra* (*BoAHL15*) were used to amplify the open reading frames using primers indicated in Supplementary Table 1. The resulting fragments were cloned into plasmid pJET1/blunt (GeneJET™ PCR Cloning Kit, #K1221), and subsequently transferred as *NotI* fragments to binary vector pGPTV 35S-FLAG (Becker et al., 1992). All binary vectors were introduced into *Agrobacterium tumefaciens* strain AGL1 by electroporation (den Dulk-Ras and Hooykaas, 1995) and *Arabidopsis* Col-0 and *ahl15* plants were transformed using the floral dip method (Clough and Bent, 1998).

Tobacco transformation

Round leaf discs were prepared from the lamina of 3rd and 4th leaves of 1-month-old soil grown tobacco plants. The leaf discs were surface sterilized by three washes with sterile water followed by incubation in 10% chlorine solution for 20 minutes, and by 4 to 5 subsequent washes with sterile water (Baltes et al., 2014). The surface sterilized leaf discs were syringe infiltrated with an overnight acetosyringone (AS)-induced culture of *Agrobacterium tumefaciens* strain AGL1 containing binary vector pSRS031 (grown to OD₆₀₀= 0.6 in the presence of 100 μM AS) carrying the *35S::AHL15-GR* construct, and co-cultivated for 3 days in the dark on co-cultivation medium (CCM), consisting of full strength MS medium (Murashige and Skoog, 1962) with 3% (w/v) sucrose (pH 5.8) solidified with 0.8 % (w/v) Diachin agar and supplemented with 2mg/l BAP, 0.2mg/l NAA and 40mg/l AS. After co-cultivation, the explants were transferred to CCM supplemented with 15mg/l phosphinothricin (ppt) for selection and 500mg/l cefotaxime to kill *Agrobacterium*. Regeneration was carried out at 24°C and 16 hours photoperiod. The regenerated transgenic shoots were rooted in big jars containing 100 ml hormone free MS medium with 15mg/l ppt and 500 mg/l cefotaxime. The rooted transgenic plants were transferred to soil and grown in a growth room at 25°C, 75% relative humidity and a 16 hours photoperiod. All the transgenic plants were checked for the presence of the T-DNA insert by PCR, using genomic DNA extracted from leaf tissues by the CTAB method (Doyle, 1990).

Histochemical staining and microscopy

Histochemical staining of transgenic lines for β-glucuronidase (GUS) activity was performed as described previously (Anandalakshmi et al., 1998). Tissues were stained for 4 hours at

37°C, followed by chlorophyll extraction and rehydration by incubation for 10 minutes in a graded ethanol series (75, 50, and 25 %). GUS stained tissues were observed and photographed using a LEICA MZ12 microscope equipped with a LEICA DC500 camera.

Quantitative real-time PCR (qPCR) analysis

RNA isolation was performed using a NucleoSpin® RNA Plant kit (MACHEREY-NAGEL). For qPCR analysis, 1 µg of total RNA was used for cDNA synthesis with the iScript™ cDNA Synthesis Kit (BioRad). PCR was performed using the SYBR-Green PCR Master mix (SYBR® Premix Ex Taq™, Takara) and a CFX96 thermal cycler (BioRad). The Pfaffl method was used to determine relative expression levels (Pfaffl, 2001). Expression was normalized using *β-TUBULIN-6* and *EF1-ALPHA* as reference genes. Three biological replicates were performed, with three technical replicates each. The primers used are described in Supplementary Table 2.

ChIP-qPCR experiment

For the ChIP-qPCR analysis, three independent samples were harvested from secondary inflorescence nodes of *pFUL:FUL-GFP ful* plants and processed as described in (Mourik et al., 2015; Balanzà et al., 2018). Primer sequences used for the ChIP-qPCR are detailed in Supplementary Table 2.

EMSA experiment

The EMSA was performed as described before (Bemer et al., 2017). The sequences of the probes are detailed in Supplementary Table 2.

AHL clade-A gene family data retrieval

The nucleotide and amino acid sequences for *AHL* clade-A genes in *A. thaliana* (*AtAHLs*) were retrieved by Biomart from Ensembl Plants (plants.ensembl.org/index.html). For our study we selected 15 additional species from 3 major plant families, i.e. Brassicaceae, Solanaceae and Fabaceae. Initially more species were included, but some were excluded from the analysis (e.g. *Arabidopsis alpina*) for reasons described below. The amino acid sequences of *A. thaliana*, *A. lyrata*, *Brassica oleracea*, *Brassica rapa*, *Solanum lycopersicum*, *Solanum tuberosum*, *Medicago truncatula* and *Glycine max* were downloaded from Ensembl Plants ([ftp://ftp.ensemblgenomes.org](http://ftp.ensemblgenomes.org)). The genomes of *Nicotiana tabacum*, *Capsicum annuum*, *Brassica napus* were downloaded from NCBI Genome ([ftp://ftp.ncbi.nih.gov/genomes/](http://ftp.ncbi.nih.gov/genomes/)) and the genomes of *Phaseolus vulgaris*, *Capsella rubella*, *Capsella grandiflora*, *Boechera stricta* and *Eutrema salsugineum* were downloaded from Phytozome (<https://phytozome.jgi.doe.gov/pz/portal.html>).

Building of profile HMMs and hmmer searches

The whole protein sequences of the Arabidopsis *AHL* clade-A genes were used as a query and BLASTP (Altschup et al., 1990) with an e-value set at 0.001 was used to search for *AHL* clade-A genes in the other plant genomes. Only BLASTP hits >70% coverage and 70% sequence identity with intact single AT-Hook motif and PPC domain were used for building profile Hidden Markov Models (HMMs). We used MAFFT software (Kato et al., 2002)

with FF-NS-i algorithm for construction of seed alignments. The alignments were manually inspected to remove any doubtful sequences. To increase the specificity of the search, columns with many gaps or low conservation were excluded using the trimAl software (Capella-gutiérrez et al., 2009). We applied a strict non-gap percentage threshold of 80% or similarity score lower than 0.001 such that at least 30% of the columns were conserved. At this point several species were excluded (e.g. *Arabidopsis thaliana*), because of extensive gaps in the sequence alignment. Profile HMMs were built from the Multiple Sequence Alignment (MSA) aligned fasta files using hmmbuild and subsequent searches against the remaining 16 genomes was carried out using hmmsearch from the HMMER 3.1b1 package (Eddy, 2011). AHL proteins in plants consist of two closely resembling clades; Clade-A and Clade-B. AHL sequences were classified to the Clade-A family based on a comparison with Clade-B AHL sequences, where a hit with lower e-value for either Clade-A or Clade-B would correctly place the sequence in the corresponding clade (e.g. low e-value for Clade A would place the sequence in Clade-A and vice-versa).

Phylogenetic reconstruction and reconciliation

Phylogenetic analysis was carried out using both Maximum Likelihood (ML) with PhyML (Guindon and Gascuel, 2003) and Bayesian Inference implementing the Markov Chain Monte Carlo (MCMC) algorithm with MrBayes (Ronquist and Huelsenbeck, 2003). For Bayesian inference, we specified the number of substitution types (nst) equal to 6 and the rate variation (rates) as invgamma. Invgamma states that a proportion of the sites are invariable while the rate for the remaining sites are drawn from a gamma distribution. These settings are equivalent to the GTR + I + gamma model. Two independent analysis (nruns=2) of 4 chains (3 heated and one cold) were run simultaneously for at least 10 million generations, sampling every 1000 generations. Burn-in was set as 25%. For Clade-A AHLs the simulations were run for 10 million generations, sampling every 1000 generations and convergence was reached at 0.016. For ML analysis, we used the default amino acid substitution model LG and the number of bootstrap replicates was specified as 100.

Tree resolving, rearrangement, and reconciliation was carried out using NOTUNG software (Liebert et al., 2000). NOTUNG uses duplication/loss parsimony to fit a gene (protein) tree to a species tree. The species tree was obtained using PhyloT (<http://phylot.biobyte.de/index.html>) which generates phylogenetic trees based on the NCBI taxonomy. Tree editing/manipulations were performed using the R packages APE (Paradis et al., 2004) and GEIGER (Harmon et al., 2008). We applied a strict threshold for rearrangement of 90%. After the rearrangement, we performed the reconciliation of the gene (protein) tree with the species tree.

Reconstruction of evolutionary scenario using Dollo parsimony method

Dollo parsimony principles are commonly exploited for two-state character traits. To classify branches as either gene-losses or gene-gains, we used Dollo parsimony method, which allows for an unambiguous reconstruction of ancestral character states, as it is based on the assumption that a complex character that has been lost during evolution of a particular lineage cannot be regained.

References

- Altschup, S.F., Gish, W., Pennsylvania, T., and Park, U.** (1990). Basic Local Alignment Search Tool 2Department of Computer Science. *J. Mol. Biol.* **215**: 403–410.
- Amasino, R.** (2009). Floral induction and monocarpic versus polycarpic life histories. *Genome Biol.* **10**: 228.
- Anandalakshmi, R., Pruss, G.J., Ge, X., Marathe, R., Mallory, A.C., Smith, T.H., and Vance, V.B.** (1998). A viral suppressor of gene silencing in plants. *Proc. Natl. Acad. Sci. U. S. A.* **22**: 13079–13084.
- Andrés, F. and Coupland, G.** (2012). The genetic basis of flowering responses to seasonal cues. *Nat. Rev. Genet.* **13**: 627–639.
- Andrés, F., Porri, A., Torti, S., Mateos, J., Romera-Branchat, M., García-Martínez, J.L., Fornara, F., Gregis, V., Kater, M.M., and Coupland, G.** (2014). SHORT VEGETATIVE PHASE reduces gibberellin biosynthesis at the Arabidopsis shoot apex to regulate the floral transition. *Proc. Natl. Acad. Sci.* **111**: E2760-9.
- Balanzà, V., Martínez-Fernández, I., Sato, S., Yanofsky, M.F., Kaufmann, K., Angenent, G.C., Bemer, M., and Ferrándiz, C.** (2018). Genetic control of meristem arrest and life span in Arabidopsis by a FRUITFULL-APETALA2 pathway. *Nat. Commun.* **9**: /s41467-018-03067-5.
- Baltes, N.J., Gil-Humanes, J., Cermak, T., Atkins, P. a, and Voytas, D.F.** (2014). DNA replicons for plant genome engineering. *Plant Cell* **26**: 151163.
- Becker, D., Kemper, E., Schell, J., and Masterson, R.** (1992). New plant binary vectors with selectable markers located proximal to the left T-DNA border. *Plant Mol. Biol.* **20**: 1195–1197.
- Bemer, M., Van Mourik, H., Muiño, J.M., Ferrándiz, C., Kaufmann, K., and Angenent, G.C.** (2017). FRUITFULL controls SAUR10 expression and regulates Arabidopsis growth and architecture. *J. Exp. Bot.* **68**: 3391–3403.
- Capella-gutiérrez, S., Silla-martínez, J.M., and Gabaldón, T.** (2009). trimAl : a tool for automated alignment trimming in large-scale phylogenetic analyses. *Bioinformatics* **25**: 1972–1973.
- Clough, S.J. and Bent, F.** (1998). Floral dip: a simplified method for Agrobacterium-mediated transformation of Arabidopsis thaliana. *Plant J.* **16**: 735–743.
- Dekker, J., Marti-Renom, M.A., and Mirny, L.A.** (2013). Exploring the three-dimensional organization of genomes: Interpreting chromatin interaction data. *Nat. Rev. Genet.* **14**: 390-403.
- Doyle, J.J.** (1990). Isolation of plant DNA from fresh tissue. *Focus (Madison).* **12**: 13–15.
- den Dulk-Ras, A. and Hooykaas, P.J.** (1995). Electroporation of Agrobacterium tumefaciens. *Methods Mol. Biol.* **55**: 63–72.
- Eddy, S.R.** (2011). Accelerated Profile HMM Searches. *PLoS Comput. Biol.* **7**.
- Grbić, V. and Bleecker, A.B.** (2000). Axillary meristem development in Arabidopsis thaliana. *Plant J.* **21**: 215–223.
- Guindon, S. and Gascuel, O.** (2003). A simple, fast, and accurate algorithm to estimate large phylogenies by maximum likelihood. *Syst. Biol.* **5**.
- Harmon, L.J., Weir, J.T., Brock, C.D., Glor, R.E., Challenger, W., and Science, A.** (2008). GEIGER : investigating evolutionary radiations. *Bioinformatics* **24**: 129–131.
- Huang, S., Raman, A.S., Ream, J.E., Fujiwara, H., Cerny, R.E., and Brown, S.M.** (1998). Overexpression of 20-Oxidase confers a gibberellin- overproduction phenotype in Arabidopsis. *Plant Physiol.* **118**: 773–781.
- Immink, R.G.H., Posé, D., Ferrario, S., Ott, F., Kaufmann, K., Valentim, F.L., de Folter, S., van der Wal, F., van Dijk, A.D.J., Schmid, M., and Angenent, G.C.** (2012). Characterization of SOC1's central role in flowering by the identification of its upstream and downstream regulators. *Plant Physiol.* **160**: 433–449.
- Karimi, M., Depicker, A., and Hilson, P.** (2007). Recombinational cloning with plant gateway vectors.

- Plant Physiol. **145**: 1144–1154.
- Katoh, K., Misawa, K., Kuma, K., and Miyata, T.** (2002). MAFFT : a novel method for rapid multiple sequence alignment based on fast Fourier transform. *Nucleic Acids Res.* **30**: 3059–3066.
- Kiefer, C., Severing, E., Karl, R., Bergonzi, S., Koch, M., Tresch, A., and Coupland, G.** (2017). Divergence of annual and perennial species in the Brassicaceae and the contribution of cis-acting variation at FLC orthologues. *Mol. Ecol.* **26**: 3437–3457.
- Ko, J., Han, K., Park, S., and Yang, J.** (2004). Plant Body Weight-Induced Secondary Growth in Arabidopsis and Its Transcription Phenotype Revealed by Whole-Transcriptome Profiling 1 [w]. *Plant Physiol.* **135**: 1069–1083.
- Lee, J. and Lee, I.** (2010). Regulation and function of SOC1 , a flowering pathway integrator. *J. Exp. Bot.* **61**: 2247–2254.
- Liebert, M.A., Chen, K., Durand, D., Farach-colton, M., and Al, C.E.T.** (2000). NOTUNG : A Program for Dating Gene Duplications. *J. Comput. Biol.* **7**: 429–447.
- Lim, P.O., Kim, Y., Breeze, E., Koo, J.C., Woo, H.R., Ryu, J.S., Park, D.H., Beynon, J., Tabrett, A., Buchanan-Wollaston, V., and Nam, H.G.** (2007). Overexpression of a chromatin architecture-controlling AT-hook protein extends leaf longevity and increases the post-harvest storage life of plants. *Plant J.* **52**: 1140–1153.
- Matsoukas, I.G., Massiah, A.J., and Thomas, B.** (2012). Florigenic and antiflorigenic signaling in plants. *Plant Cell Physiol.* **53**: 1827–1842.
- Matsushita, A., Furumoto, T., Ishida, S., and Takahashi, Y.** (2007). AGF1, an AT-hook protein, is necessary for the negative feedback of AtGA3ox1 encoding GA 3-oxidase. *Plant Physiol.* **143**: 1152–1162.
- Melzer, S., Lens, F., Gennen, J., Vanneste, S., Rohde, A., and Beeckman, T.** (2008). Flowering-time genes modulate meristem determinacy and growth form in Arabidopsis thaliana. *Nat. Genet.* **40**: 1489–1492.
- Mourik, H. Van, Muiño, J.M., Pajoro, A., Angenent, G.C., and Kaufmann, K.** (2015). Characterization of In Vivo DNA-Binding Events of Plant Transcription Factors by ChIP-seq : Experimental Protocol and Computational Analysis. *Methods Mol Biol* **1284**: 93–121.
- Munné-Bosch, S.** (2008). Do perennials really senesce? *Trends Plant Sci.* **13**: 216–220.
- Murashige, T. and Skoog, F.** (1962). A Revised Medium for Rapid Growth and Bio Assays with Tobacco Tissue Cultures. *Physiol. Plant.* **15**: 473–497.
- Ng, K.-H., Yu, H., and Ito, T.** (2009). AGAMOUS controls GIANT KILLER, a multifunctional chromatin modifier in reproductive organ patterning and differentiation. *PLoS Biol.* **7**: e1000251.
- Paradis, E., Claude, J., and Strimmer, K.** (2004). APE : Analyses of Phylogenetics and Evolution in R language. *Bioinformatics* **20**: 289–290.
- Park, S.J., Eshed, Y., and Lippman, Z.B.** (2014). Meristem maturation and inflorescence architecture — lessons from the Solanaceae. *Curr. Opin. Plant Biol.* **17**: 70–77.
- Passarinho, P., Ketelaar, T., Xing, M., van Arkel, J., Maliepaard, C., Hendriks, M.W., Joosen, R., Lammers, M., Herdies, L., den Boer, B., van der Geest, L., and Boutilier, K.** (2008). BABY BOOM target genes provide diverse entry points into cell proliferation and cell growth pathways. *Plant Mol. Biol.* **68**: 225–237.
- Pfaffl, M.W.** (2001). A new mathematical model for relative quantification in real-time RT-PCR. *Nucleic Acids Res.* **29**: e45--e45.
- Remington, D.L., Figueroa, J., and Rane, M.** (2015). Timing of shoot development transitions affects degree of perenniality in Arabidopsis lyrata (Brassicaceae). *BMC Plant Biol.* **15**: 1–13.
- Rieu, I., Ruiz-Rivero, O., Fernandez-Garcia, N., Griffiths, J., Powers, S.J., Gong, F., Linhartova, T., Eriksson, S., Nilsson, O., Thomas, S.G., Phillips, A.L., and Hedden, P.** (2008). The gibberellin biosynthetic genes AtGA20ox1 and AtGA20ox2 act, partially redundantly, to promote growth and development throughout the Arabidopsis life cycle. *Plant J.* **53**: 488–504.
- Ronquist, F. and Huelsenbeck, J.P.** (2003). MrBayes 3 : Bayesian phylogenetic inference under mixed models. *Bioinformatics* **19**: 1572–1574.
- Song, Y.H., Ito, S., and Imaizumi, T.** (2013). Flowering time regulation: photoperiod- and

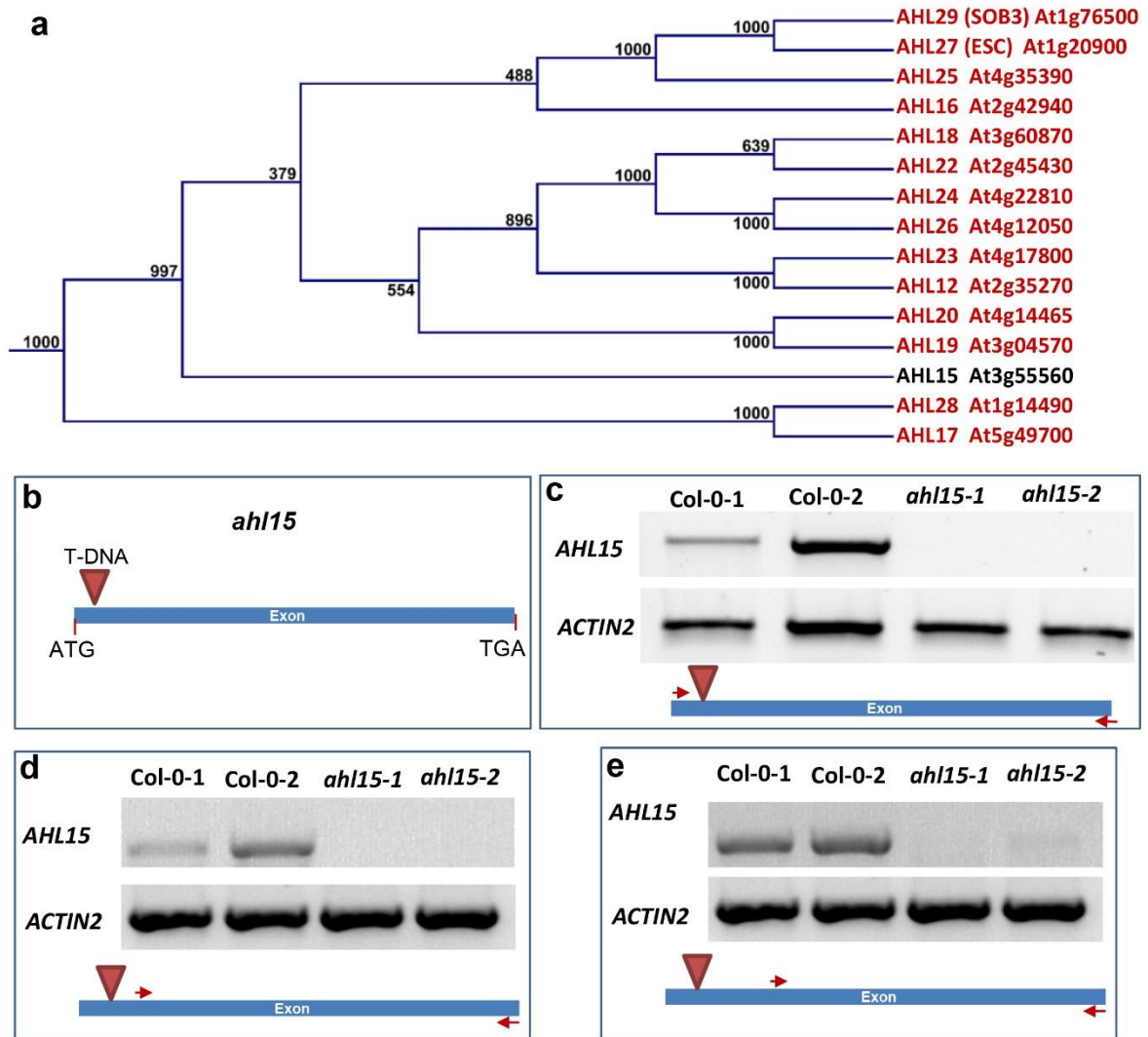
- temperature-sensing in leaves. *Trends Plant Sci.* **18**: 575–583.
- Street, I.H., Shah, P.K., Smith, A.M., Avery, N., and Neff, M.M.** (2008). The AT-hook-containing proteins SOB3/AHL29 and ESC/AHL27 are negative modulators of hypocotyl growth in *Arabidopsis*. *Plant J.* **54**: 1–14.
- Tao, Z., Shen, L., Liu, C., Liu, L., Yan, Y., and Yu, H.** (2012). Genome-wide identification of SOC1 and SVP targets during the floral transition in *Arabidopsis*. *Plant J.* **70**: 549–561.
- Tilmes, V., Mateos, J.L., Madrid, E., Vincent, C., Severing, E., Carrera, E., López-Díaz, I., and Coupland, G.** (2019). Gibberellins Act Downstream of *Arabidopsis* PERPETUAL FLOWERING1 to Accelerate Floral Induction during Vernalization. *Plant Physiol.* **180**: 1549–1563.
- Turnbull, C.** (2011). Long-distance regulation of flowering time. *J. Exp. Bot.* **62**: 4399–43413.
- Wang, B., Smith, S.M., and Li, J.** (2018). Genetic Regulation of Shoot Architecture. *Annu. Rev. Plant Biol.* **69**: 437–468.
- Wang, J.-W.** (2014). Regulation of flowering time by the miR156-mediated age pathway. *J. Exp. Bot.* **65**: 4723–4730.
- Wang, J.-W., Czech, B., and Weigel, D.** (2009). miR156-regulated SPL transcription factors define an endogenous flowering pathway in *Arabidopsis thaliana*. *Cell* **138**: 738–749.
- Xiao, C., Chen, F., Yu, X., Lin, C., and Fu, Y.-F.** (2009). Over-expression of an AT-hook gene, AHL22, delays flowering and inhibits the elongation of the hypocotyl in *Arabidopsis thaliana*. *Plant Mol. Biol.* **71**: 39–50.
- Yu, S., Galvão, V.C., Zhang, Y.-C., Horrer, D., Zhang, T.-Q., Hao, Y.-H., Feng, Y.-Q., Wang, S., Schmid, M., and Wang, J.-W.** (2012). Gibberellin regulates the *Arabidopsis* floral transition through miR156-targeted SQUAMOSA promoter binding-like transcription factors. *Plant Cell* **24**: 3320–32.
- Yun, J., Kim, Y.-S., Jung, J.-H., Seo, P.J., and Park, C.-M.** (2012). The AT-hook motif-containing protein AHL22 regulates flowering initiation by modifying FLOWERING LOCUS T chromatin in *Arabidopsis*. *J. Biol. Chem.* **287**: 15307–16.
- Zhao, J., Favero, D.S., Peng, H., and Neff, M.M.** (2013). *Arabidopsis thaliana* AHL family modulates hypocotyl growth redundantly by interacting with each other via the PPC/DUF296 domain. *Proc. Natl. Acad. Sci.* **110**: E4688–E4697.
- Zhao, J., Favero, D.S., Qiu, J., Roalson, E.H., and Neff, M.M.** (2014). Insights into the evolution and diversification of the AT-hook Motif Nuclear Localized gene family in land plants. *BMC Plant Biol.* **14**: 266.

Acknowledgments

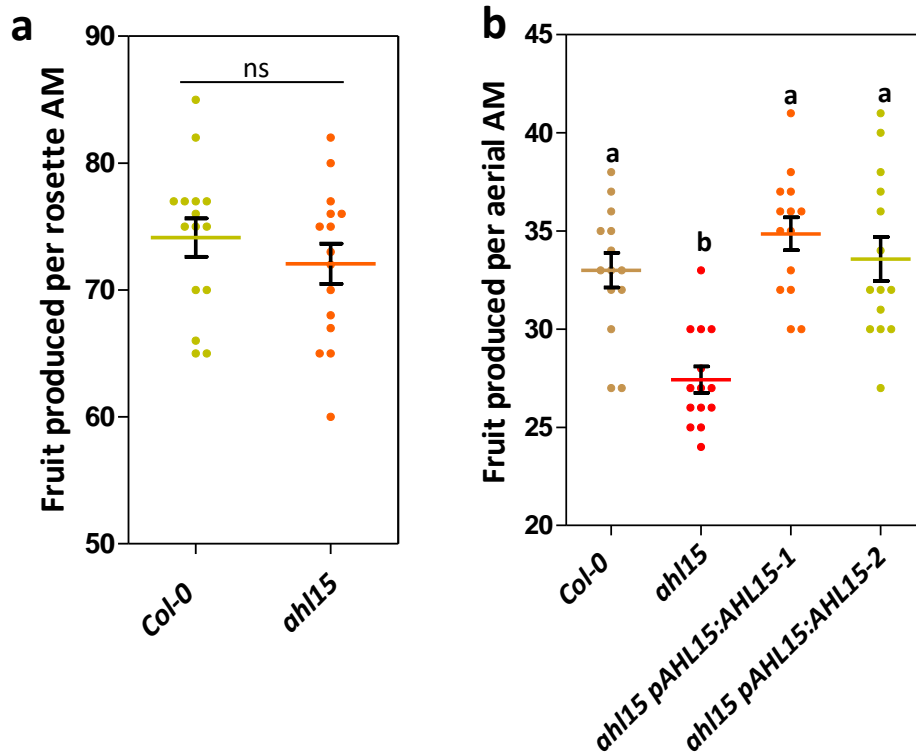
We thank Kim Boutilier and Thomas Greb for critical comments on the manuscript.

Author contribution

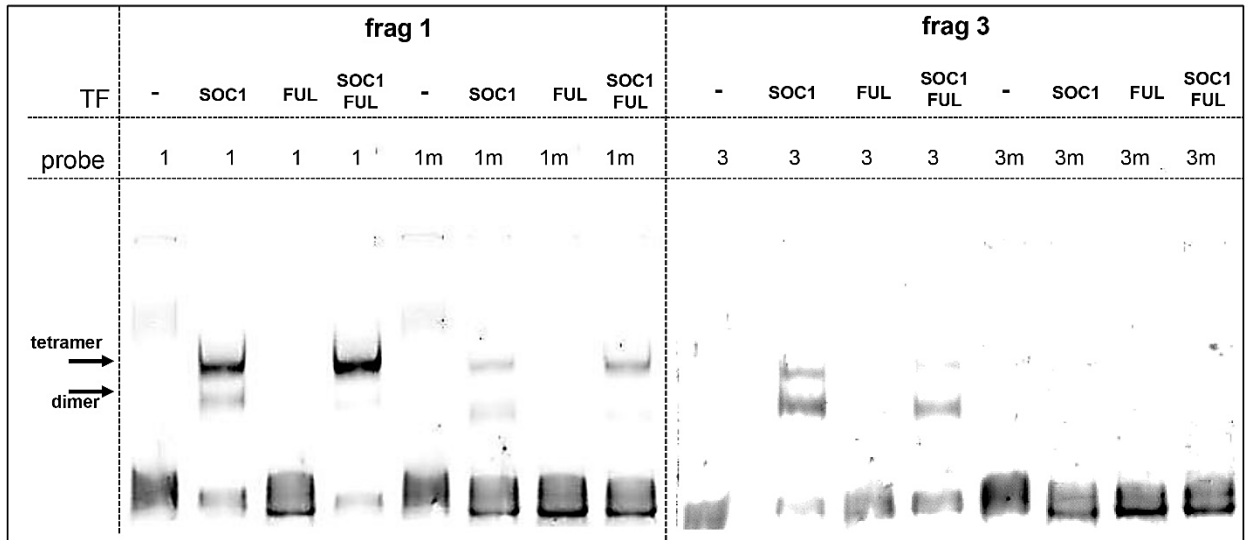
O.K. and R.O. conceived and supervised the project; O.K. and A.R. performed respectively 50% and 40% of the *Arabidopsis* experiments. All authors designed experiments and analyzed and interpreted results; O.K. and A.R. performed the majority of the *Arabidopsis* experiments; M.B., P.M., and M.C. contributed to the *Arabidopsis* experiments; M.K. generated and analyzed the tobacco lines; R.R.H. and V.N. analysed the *AHL* gene families in different mono- and polycarpic plant species, O.K., A.R and R.O. wrote the manuscript; All authors read and commented on versions of the manuscript.



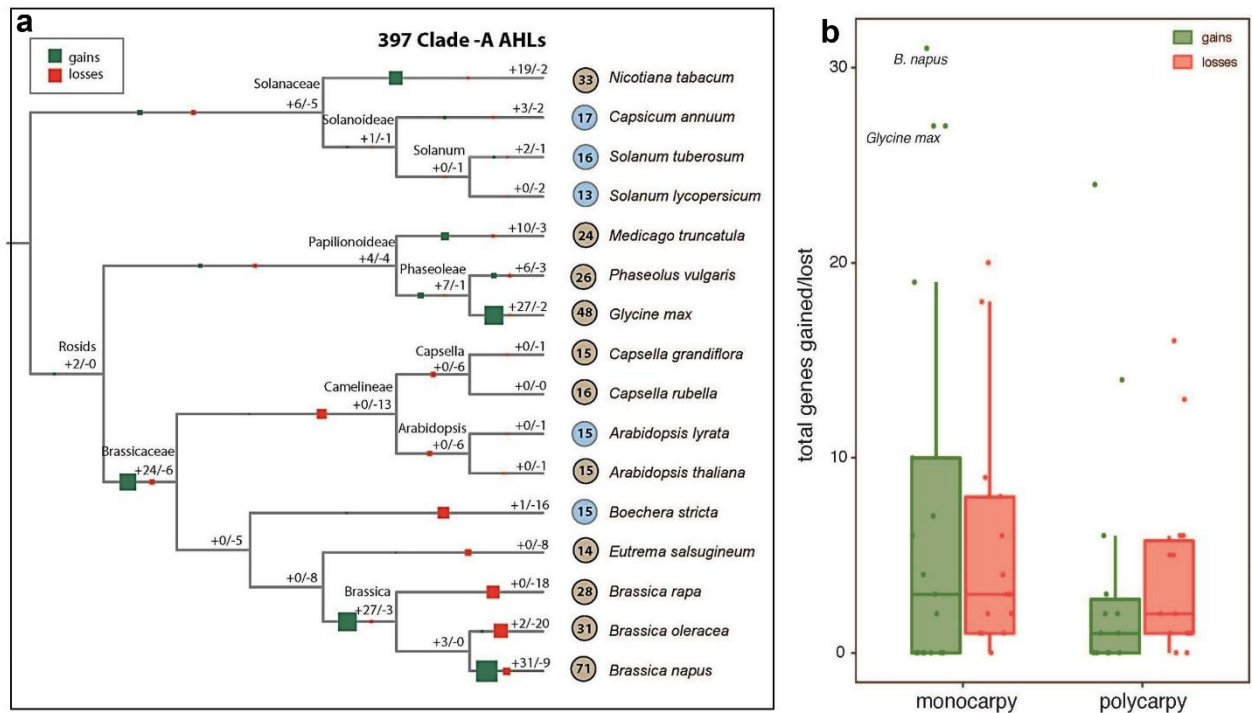
Supplementary Fig. 1 | The Arabidopsis clade-A AHL protein and gene family. (a) A phylogenetic tree of part of the Arabidopsis AHL protein family showing all clade-A AHL proteins containing a single At-Hook domain, including AHL15. (b) Location of the T-DNA insertion in the intronless *AHL15* gene, resulting in the *ahl15* loss-of-function mutant allele used for this research. (c-e) Duplicate RT-PCR detection of full-length *AHL15* coding sequence (CDS) (c), from 64bp downstream of the ATG until the end of the CDS (d) and from 197bp downstream of the ATG until end of the CDS (e) in wild-type Arabidopsis (Col-0) but not in the *ahl15* mutant. The *ACTIN2* was used as a positive control. The primers used for RT-PCR are described in Supplementary Table 2.



Supplementary Fig. 2 | Repression of AM maturation by *AHL15* leads to increased flower and fruit production in *Arabidopsis*. (a) The number of fruits produced by the rosette AMs of 7-week-old wild-type or *ahl15* plants. Dots indicate number of fruits produced per AM per plant (n=15 biologically independent plants), horizontal lines indicate the mean, and error bars the SEM. ns indicates no significant difference ($p < 0.05$), as determined by a two-sided Student's *t*-test. The P values are provided in Supplementary Table 18. (b) The number of fruits produced by the aerial AMs of 7-week-old wild-type, *ahl15* or *ahl15 pAHL15:AHL15* plants. Dots indicate number of fruits produced per AM per plant (n=15 biologically independent plants), horizontal lines indicate the mean, and error bars the SEM. Letters (a, b) indicate statistically significant differences ($p < 0.01$), as determined by a one-way ANOVA with a Tukey's HSD post hoc test.

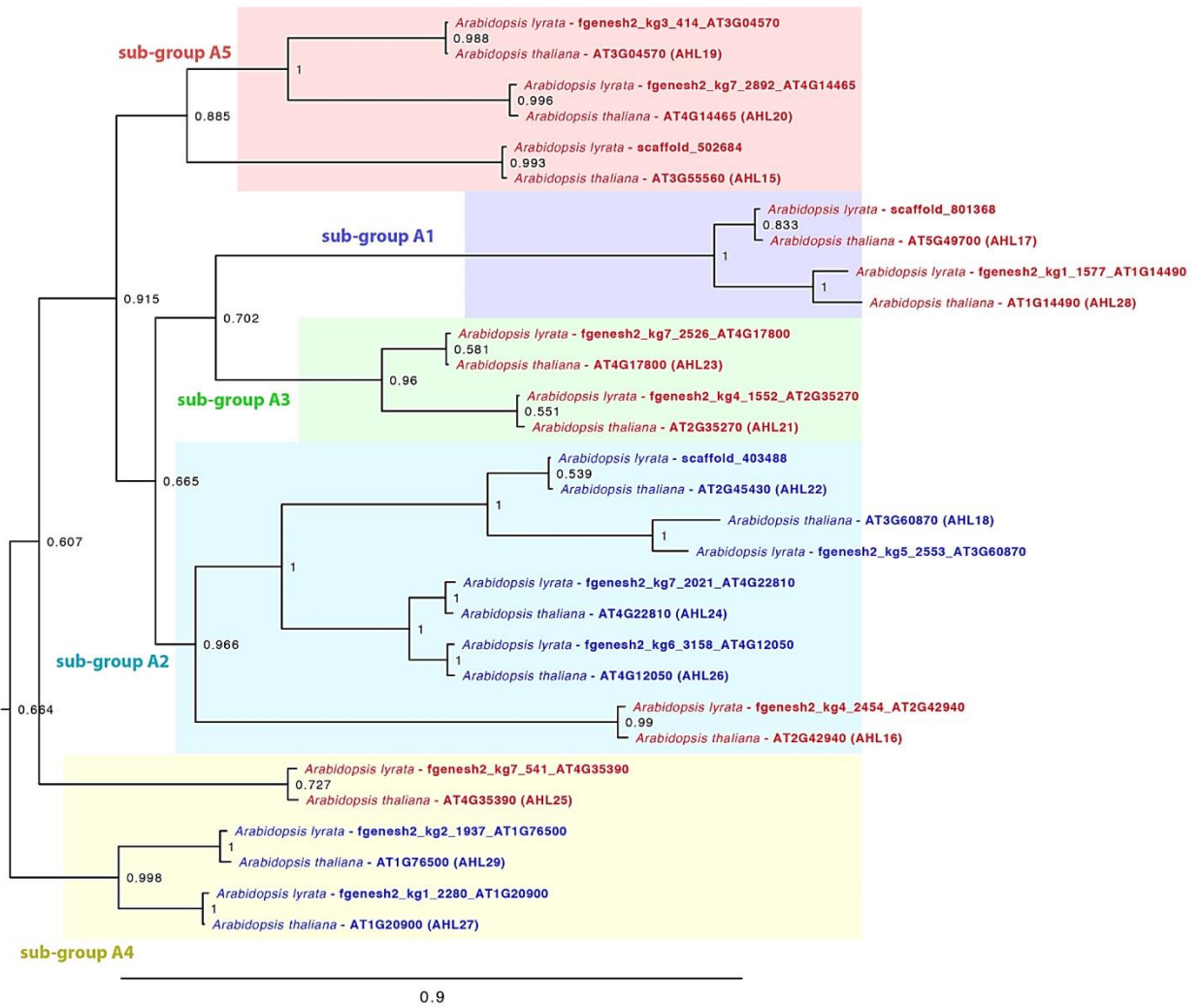


Supplementary Fig. 3. Binding of SOC1 and FUL to regulatory regions near *AHL15*. Left panel: EMSA of promoter fragment 1 with a wild-type (1) or mutated (m1) CArG-box. Right panel: EMSA of downstream fragment 3 with a wild-type (3) or mutated (3m) CArG-box. Shifting of the probe, indicating binding, occurs either by a tetramer (upper band) or dimer (lower band).



Supplementary Figure 4. Evolutionary history of the Clade-A *AHL* gene family in relation to the monocarpic and polycarpic plant growth habit. (a) Reconciliation of the gene (protein) tree with the species tree of 16 selected dicot plant species with either a monocarpic (light brown circled number) or a polycarpic (light blue circled number) life history strategy. The tree topology was extracted from the NCBI taxonomy database. For each tree node, the number of gained genes (+) is indicated by the size of the green box, and the number of lost genes (-) by the size of the red box. The total number of *AHL* genes for each plant species is indicated by the circled number. (b) The distribution of total Clade-A *AHL* gene gains and losses for monocarpic or polycarpic in (a) have been summarized as box-plots. The character state of each ancestor was determined for the presence (polycarpic) or absence (monocarpic) of polycarpic growth habit using Dollo's parsimony principle. Horizontal bars indicate median values, boxes demarcate 1st and 3rd quartiles, and whiskers delineate minimum (within 1.5 times Inter Quartile Range (IQR) below 1st quartile) and maximum (within 1.5 times IQR above 3rd quartile) values. The dots in the box-plots indicate all the ancestral states and current species for which the total gene gains/losses were estimated (n = 11 monocarpic species and 5 polycarpic species). The outlier species are labelled with the species name. The outlier species are labelled with the species name.

A suppressor of axillary meristem maturation promotes longevity in flowering..



Supplementary Fig. 5 | Phylogenetic tree of *A. thaliana* and *A. lyrata* clade-A AHL proteins. The tree shows 15 one-to-one orthologous pairs between the two species.

Supplementary Table 1: PCR primers used for cloning and genotyping

Name*	Sequence (5' to 3')	Purpose
Gateway-AHL15-F	GGGGACAAGTTTGTACAAAAAAGCAGGCTCGATGGCGAATCCTTGGTGGGT	<i>pGW-AHL15</i> construct
Gateway-AHL15-R	GGGGACCACTTTGTACAAGAAAGCTGGGTAATACGAAGGAGGAGCACGAG	
ccdB gene +KpnI-F	CGGGTACCGCTATCGAACCACCTTTGTAC	Amplify <i>ccdB</i> gene
ccdB gene +SphI-R	GACTGCAAGTCACGTCGGCAG	
pAHL15:AHL15-F	GGGGACAAGTTTGTACAAAAAAGCAGGCTCGACACTCCTCTGTGCCACATT	<i>pAHL15:AHL15</i> construct
pAHL15:AHL15-R	GGGGACCACTTTGTACAAGAAAGCTGGGTATCTTTTTTCTCTCTAATGG	
pFD:AHL15-F	GGGGACAAGTTTGTACAAAAAAGCAGGCTGGCCCTCTACTTGATTAG	<i>pFD:AHL15</i> construct
pFD:AHL15-R	GGGGACCACTTTGTACAAGAAAGCTGGGTATGGAAAAGAGAACAGAAAGTGAAC	
pMYB85:AHL15-F	GGGGACAAGTTTGTACAAAAAAGCAGGCTGGTGGGGTGTGAAATGTCAC	<i>pMYB85:AHL15</i> construct
pMYB85:AHL15-R	GGGGACCACTTTGTACAAGAAAGCTGGGTATAAATACTATATAGAAATGATATG	
pMYB103:AHL15-F	GGGGACAAGTTTGTACAAAAAAGCAGGCTTCTATTGCTCCTCTAAAGG	<i>pMYB103:AHL15</i> construct
pMYB103:AHL15-R	GGGGACCACTTTGTACAAGAAAGCTGGGTAGATTAGTAGCTCCTCAAAGTAAC	
p35S:AHL29-F	ATAAGAATGCGGCCGCGACGGTGGTTACGATCAATC	<i>p35S:AHL29</i> construct
p35S:AHL29-R	ATAGTTTAGCGGCCGCTAAAAGGCTGGTCTTGGTG	
p35S:AHL20 -F	ATAAGAATGCGGCCGCGCAAACCCTTGGTGGACGAAC	<i>p35S:AHL20</i> construct
p35S:AHL20-R	ATAGTTTAGCGGCCGCTCAGTAAGGTGGTCTTGCCT	
p35S:AHL27-F	ATAAGAATGCGGCCGCGAAGGCGGTTACGAGCAAGG	<i>p35S:AHL27</i> construct
p35S:AHL27-R	ATAGTTTAGCGGCCGCTTAAAAAGGTGGTCTTGAAG	
p35S: BoAHL15-1-F	ATAAGAATGCGGCCGCGCAATCCTTGGTGGGTAGA	<i>p35S:BoAHL15</i> construct
p35S: BoAHL15-1-R	ATAGTTTAGCGGCCGCTCAATATGAAGGAGGACCAC	
p35S: MtAHL15-F	ATAAGAATGCGGCCGCTCGAATCGATGGTGGAGTGG	<i>p35S: MtAHL15</i> construct
p35S: MtAHL15-R	ATAGTTTAGCGGCCGCTCAATATGGAGGTGGATGTG	
p35S:AHL19-F	GGGGACAAGTTTGTACAAAAAAGCAGGCTCGATGGCGAATCCATGGTGGAC	<i>p35S:AHL19</i> construct
p35S:AHL19-R	GGGGACCACTTTGTACAAGAAAGCTGGGTAACAAGTAGCAACTGACTGG	
SALK_040729-F	GTCGGAGAGCCATCAACACCA	<i>ahl15</i> genotyping
SALK_040729-R	CGACGACCCGTAGACCCGGATC	
soc1-6 -F	AAAGGATGAGGTTTCAAGCG	<i>soc1-6</i> genotyping
soc1-6 -R	ATGTGATTCCACAAAAGGCC	
ful-7-F	TTTCCGCCTTCTCTCGTTGTG	<i>ful-7</i> genotyping

*, F: forward; R: reverse

Supplementary Table 2: PCR primers used for qRT-PCR and RT-PCR

Name*	Sequence (5' to 3')	Purpose
qAHL15-F	AAGAGCAGCCGCTTCAACTA	<i>qRT-PCR AHL15</i>
qAHL15-R	TGTTGAGCCATTTGATGACC	
qAHL16-F	CCAGCTTCATCAGGAGCAAT	<i>qRT-PCR AHL16</i>
qAHL16-R	ATGCAGCCATGAGAACAACA	
qAHL17-F	GTCCACTTATTTCCGGCAGGA	<i>qRT-PCR AHL17</i>
qAHL17-R	TACCCACACGACTCTCCTC	
qAHL18-F	ACACGGACGGTTTGAGATTC	<i>qRT-PCR AHL18</i>
qAHL18-R	GCCTCTCGTAAGATGCGTTT	
qAHL19-F	CTCTAACGCGACTTACGAGAGATT	<i>qRT-PCR AHL19</i>
qAHL19-R	ATATTATACACCGGAAGTCCTTGGT	
qAHL20-F	CAAGGCAGGTTTGAATCTTATCT	<i>qRT-PCR AHL20</i>
qAHL20-R	TAGCGTTAGAGAAAGTAGCAGCAA	
qAHL22-F	AGCTGGAGCGGTTGCTAATA	<i>qRT-PCR AHL22</i>
qAHL22-R	CAGCTGGCAATTGAACAGAA	
qAHL23-F	TTGTGACGCTACAAGGAACG	<i>qRT-PCR AHL23</i>
qAHL23-R	AAACGAAGCTGCAATCACAA	
qAHL24-F	TGGTTGGAGGAAGCGTAGTT	<i>qRT-PCR AHL24</i>
qAHL24-R	GCTTGTGCTGATGTTGCAG	
qAHL25-F	GCAAACGCAGTTTATGATAGGTTAC	<i>qRT-PCR AHL25</i>
qAHL25-R	ATTCCAAGATTGTAGAAAGCAACAC	
qAHL26-F	GGTGGGACCTTTGTTGTGTT	<i>qRT-PCR AHL26</i>
qAHL26-R	TGCCATAGCTTGTGCTGTC	
R ₁ AHL15-F	ATGGCGAATCCTTGGTGGGTAG	<i>RT-PCR₁ AHL15</i>
R ₁ AHL15-R	TCAATACGAAGGAGGAGCAGGAG	
R ₁ ACTIN2-F	TGAGACCTTAACTCTCCCGCTA	<i>RT-PCR ACTIN2</i>
R ₁ ACTIN2-R	TGATTTCTTTGCTCATAACGGTCA	
R ₂ AHL15-F	TCAGCT CCT TCT TTGCACCAC	<i>RT-PCR₂ AHL15</i>
R ₂ AHL15-R	ATACGAAGGAGGAGCAGCAGG	
R ₃ AHL15-F	AAGAACAGAACAGCAGAGACG	<i>RT-PCR₃ AHL15</i>
R ₃ AHL15-R	TCAATACGAAGGAGGAGCAGC	
qβ-TUBULIN-6-F	TGGGAACCTCTGCTCATATCT	<i>qRT-PCR AHL15</i>
qβ-TUBULIN-6-R	GAAAGGAATGAG GTTCACTG	
QEF1ALPHA-F	TGAGCACGCTCTTCTTGCTTTCA	<i>qRT-PCR EF1alpha</i>
QEF1ALPHA-R	GGTGGTGGCATCCATCTTGTTACA	
ChIP REF1-F	TCTCCGACCTTTCTTCACACCCATTCC	<i>ChIP-qPCR REF1</i>
ChIP REF1-R	CTGAGAACTTGCTTACTTGTAGACTC	
ChIP REF2-F	GCTATCCACAGGTTAGATAAAGGAG	<i>ChIP-qPCR REF2</i>
ChIP REF2-R	GGACTAGATTTGAGGAAAGGAAGGA	
ChIP frag1-F	TGTCACACCACTCTCTTTGCA	<i>ChIP-qPCR frag1</i>
ChIP frag1-R	AATAATGGTTACTGAAAACGTACA	
ChIP exon-F	TCCAGAGCCATGTTCTTGAG	<i>ChIP-qPCR exon</i>
ChIP exon-R	GCTGACGCAGAGTAACATTAG	
ChIP frag3-F	TTGGATCTTTGGCATTGTCTC	<i>EMSA-PCR frag3</i>
ChIP frag3-R	TGCTACGGAGTTTAGTCATCA	
EMSA frag1-F	TGTCACACCACTCTCTTTGCA	<i>PCR frag1</i>
EMSA frag1-R	AATAATGGTTACTGAAAACGTACA	
EMSA exon-F	TCCAGAGCCATGTTCTTGAG	<i>PCR exon</i>
EMSA exon-R	GCTGACGCAGAGTAACATTAG	
EMSA frag3-F	TTGGATCTTTGGCATTGTCTC	<i>PCR frag3</i>
EMSA frag3-R	TGCTACGGAGTTTAGTCATCA	
EMSA frag1 sequence	TGTCACACCACTCTCTTTGCA AAAAAATAACAGCCCTTATTTGGATCTTACAATAAATGTACGTTTTCAGTAACCA TTATT	
EMSA mutated frag1 sequence	TGTCACACCACTCTCTTTGCA AAAAAATAACAGCCCTTCTTTGGATCTTACAATAAATGTACGTTTTCAGTAACCA TTATT	
EMSA exon sequence	TTGGATCTTTGGCATTGTCTCTGGTCTTAAATATCCCTTTTATGGTATATCAAAAA AACATGAGTACGGAATATATGGTCCCATGATGACTAAACTCCGTAGCA	

Chapter 2

EMSA frag3 sequence	TTGGATCTTTGGCATTGTCTCTGGTCTTAAATATCCCCTCCATGGTATATCAAAAA AACATGAGTACGGAATATATGGTCCCATGATGACTAAACTCCGTAGCA
EMSA mutated frag3 sequence	TCCAGAGCCATGTTCTTGAGATTGCTACGGGAGCTGACGTGGCGGAAAGCTTAA ACGCCTTGCTCGTAGACGCGGCCGGGGCGTTTCGGTGCTGAGCGGTAGTGGTTT GGTACTAATGTTACTCTGCGTCAGC

*, F: forward; R: reverse.

